

**$Z_c$ -like spectra from QCD Laplace sum rules at NLO**R. M. Albuquerque<sup>†</sup>*Faculty of Technology, Rio de Janeiro State University (FAT, UERJ), Brazil*S. Narison<sup>\*,‡</sup>*Laboratoire Univers et Particules de Montpellier (LUPM) CNRS-IN2P3  
and University of Montpellier Case 070, Place Eugène Bataillon, Montpellier 34095, France  
and Institute of High-Energy Physics of Madagascar (iHEPMAD) University of Ankatso,  
Antananarivo 101, Madagascar*D. Rabetiarivony<sup>§</sup>*Institute of High-Energy Physics of Madagascar (iHEPMAD) University of Ankatso,  
Antananarivo 101, Madagascar* (Received 17 January 2021; accepted 16 March 2021; published 22 April 2021)

We present a global analysis of the observed  $Z_c$ ,  $Z_{cs}$ , and future  $Z_{css}$ -like spectra using (inverse) Laplace sum rule within stability criteria. Integrated compact QCD expressions of the leading order spectral functions up to dimension-six condensates are given. Next-to-leading order factorized perturbative contributions are included. We reemphasize the importance to include perturbative radiative corrections (though numerically small) for heavy quark sum rules in order to justify the (ad hoc) definition and value of the heavy quark mass used frequently at leading order in the literature. We also demonstrate that, contrary to a qualitative large  $N_c$  counting, the two-meson scattering contributions to the four-quark spectral functions are numerically negligible confirming the reliability of the Laplace sum rule predictions. Our results are summarized in Tables III to VI. The  $Z_c(3900)$  and  $Z_{cs}(3983)$  spectra are well reproduced by the  $T_c(3900)$  and  $T_{cs}(3973)$  tetramoles (superposition of quasidegenerated molecules and tetraquark states having the same quantum numbers and with almost equal couplings to the currents). The  $Z_c(4025)$  or  $Z_c(4040)$  state can be fitted with the  $D_0^*D_1$  molecule having a mass 4023(130) MeV while the  $Z_{cs}$  bump around 4.1 GeV can be likely due to the  $D_{s0}^*D_1 \oplus D_0^*D_{s1}$  molecules. The  $Z_c(4430)$  could be a radial excitation of the  $Z_c(3900)$  weakly coupled to the current, while all strongly coupled ones are in the region (5634 ~ 6527) MeV. The double strange tetramole state  $T_{css}$ , which one may identify with the future  $Z_{css}$ , is predicted to be at 4064(46) MeV. It is remarkable to notice the regular mass splittings of the tetramoles due to  $SU(3)$  breakings:  $M_{T_{cs}} - M_{T_c} \approx M_{T_{css}} - M_{T_{cs}} \simeq (73 \sim 91)$  MeV.

DOI: 10.1103/PhysRevD.103.074015

**I. INTRODUCTION**

Beyond the successful quark model of Gell-Mann [1] and Zweig [2], Rossi and Veneziano have introduced the four-quark states within the string model [3] in order to describe baryon-antibaryon scattering, while Jaffe [4] has

introduced them within the bag models for an attempt to explain the complex structure of the  $I = 1, 0$  light scalar mesons (see also [5–7]).

In earlier papers, QCD spectral sum rules (QSSR) has been used to estimate the  $I = 0$  light scalar mesons ( $\sigma, f_0$ ) masses and widths [8] assumed to be four-quark states. However, the true nature of these states remains still an open question as they can be well interpreted as glueballs/gluonia [9–12].

After the recent discovery of many exotic XYZ states beyond the quark model found in different accelerator experiments,<sup>1</sup> there was a renewed interest on the four-quarks and molecule states for attempting to explain the properties of these new exotic states.<sup>2</sup>

\*Corresponding author.

snarison@yahoo.fr

†raphael.albuquerque@uerj.br

‡ICTP-Trieste consultant for Madagascar

§rd.bidds@gmail.com

Published by the American Physical Society under the terms of the [Creative Commons Attribution 4.0 International license](https://creativecommons.org/licenses/by/4.0/). Further distribution of this work must maintain attribution to the author(s) and the published article's title, journal citation, and DOI. Funded by SCOAP<sup>3</sup>.

<sup>1</sup>For a recent review, see, e.g., [13].<sup>2</sup>For reviews, see, e.g., [3,14–21].

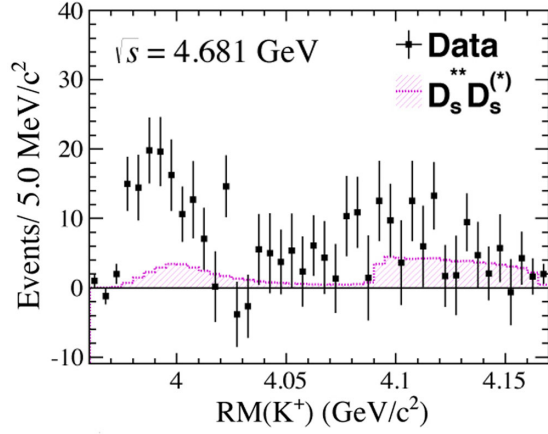


FIG. 1.  $K^+$  recoil mass at  $\sqrt{s} = 4.681$  GeV after background subtractions from BESIII [45].

In previous works [22–24], we have systematically extracted the couplings and masses of the XYZ states using QSSR à la Shifman-Vainshtein-Zakharov (SVZ) [25,26]<sup>3</sup> where the next-to-next-to-leading-order factorized perturbative and QCD condensates up to dimension-6 in the operator product expansion (OPE) corrections have been included.<sup>4</sup> In so doing, we have used the inverse Laplace transform [38–40] version of QSSR within stability criteria where we have emphasized the importance of the perturbative (PT) corrections for giving a meaning on the input heavy quark mass value which plays an important role in the analysis, though these corrections are numerically small, within the  $\overline{\text{MS}}$  scheme.

More recently, we have applied the Laplace sum rules (LSR) for interpreting the new states around (6.2–6.9) GeV found by the LHCb group [41] to be a doubly/fully hidden-charm molecules ( $\bar{Q}Q$ )( $Q\bar{Q}$ ) and ( $\bar{Q}\bar{Q}$ )( $QQ$ ) tetraquarks states [42], while the new states found by the same group from the  $DK$  invariant mass [43] have been interpreted by a  $0^+$  and  $1^-$  tetramoles (superposition of almost degenerate molecules and tetraquark states having the same quantum numbers and couplings) slightly mixed with their radial excitations [44].

In this paper, we pursue the analysis using LSR by studying the recent data from BESIII where the  $K^+$  recoil or invariant  $D_s^*D \oplus D^*D_s$  mass (see Fig. 1) [45] is a good  $Z_{cs}(1^+)$ -like state candidate. A narrow peak is experimentally found at (in units of MeV):

$$M = (3982.5^{+1.8}_{-2.6} \pm 2.1), \quad \Gamma = (12.8^{+5.3}_{-4.4} \pm 3.0). \quad (1)$$

<sup>3</sup>For reviews, see, e.g., [27–37].

<sup>4</sup>For a recent review on the uses of QSSR for exotic hadrons, see, e.g., [14] where different leading order (LO) results are quoted.

## II. THE INVERSE LAPLACE SUM RULES

### A. The QCD molecule and tetraquarks currents

We shall be concerned with the QCD local currents  $\mathcal{O}_H^\mu(x)$  of dimension six given in Table I for  $1^+$  axial-vector molecules and tetraquarks where  $q \equiv u, s$ .  $b$  is a free mixing parameter where its optimal value was found to be zero [23,24]. The appropriate  $1^+$  hadron  $\mathcal{H}$  couples to the current as

$$\langle 0 | \mathcal{O}_H^\mu(x) | \mathcal{H} \rangle = f_{\mathcal{H}} M_{\mathcal{H}}^5 e^{\mu}, \quad (2)$$

where  $f_{\mathcal{H}}$  is the hadron decay constant analog to  $f_\pi$  and  $e^\mu$  is the axial-vector polarization. In general, the four-quark operators mix under renormalization and acquire anomalous dimensions [46]. In the present case where the interpolating currents are constructed from bilinear (pseudo)scalar currents, the anomalous dimension can be transferred to the decay constants as

$$f_{\mathcal{H}}(\mu) = \hat{f}_{\mathcal{H}}(-\beta_1 a_s)^{2/\beta_1} (1 - k_f a_s), \quad (3)$$

where  $\hat{f}_{\mathcal{H}}$  is the renormalization group invariant coupling and  $-\beta_1 = (1/2)(11 - 2n_f/3)$  is the first coefficient of the QCD  $\beta$  function for  $n_f$  flavors.  $a_s \equiv (\alpha_s/\pi)$  is the QCD coupling.  $k_f = 1.014$  for  $n_f = 4$  flavors.

### B. Form of the sum rules

We shall work with the finite energy version of the QCD inverse LSR and their ratios:

$$\begin{aligned} \mathcal{L}_n^c(\tau, \mu) &= \int_{t_0}^{t_c} dt t^n e^{-t\tau} \frac{1}{\pi} \text{Im} \Pi_{\mathcal{H}}^{(1)}(t, \mu), \\ \mathcal{R}_n^c(\tau) &= \frac{\mathcal{L}_{n+1}^c}{\mathcal{L}_n^c}, \end{aligned} \quad (4)$$

TABLE I. ( $1^+$ ) molecules and tetraquarks currents ( $q \equiv u, s$ ).

Molecules	Currents
$D_q^* D$	$(\bar{c} \gamma_\mu q)(\bar{u} i \gamma_5 c)$
$D^* D_q$	$(\bar{u} \gamma_\mu c)(\bar{c} i \gamma_5 q)$
$D_{q_0}^* D_1$	$(\bar{c} q)(\bar{u} \gamma_\mu \gamma_5 c)$
$D_0^* D_{q_1}$	$(\bar{u} c)(\bar{c} \gamma_\mu \gamma_5 q)$
$D_s^* D_s$	$(\bar{c} \gamma_\mu s)(\bar{s} i \gamma_5 c)$
$D_{s_0}^* D_{1s}$	$(\bar{c} s)(\bar{s} \gamma_\mu \gamma_5 c)$
Tetraquarks	Currents
$A_{cq}$	$\epsilon_{ijk} \epsilon_{mnk} [(q_i^T C \gamma_5 c_j)(\bar{u}_m \gamma_\mu C \bar{c}_n^T) + b(q_i^T C c_j)(\bar{u}_m \gamma_\mu \gamma_5 C \bar{c}_n^T)]$
$A_{css}$	$\epsilon_{ijk} \epsilon_{mnk} [(s_i^T C \gamma_5 c_j)(\bar{s}_m \gamma_\mu C \bar{c}_n^T) + b(s_i^T C c_j)(\bar{s}_m \gamma_\mu \gamma_5 C \bar{c}_n^T)]$

where  $m_c$  is the charm quark mass,  $\tau$  is the LSR variable,  $n = 0, \dots$  is the degree of moments,  $t_0$  is the quark/hadronic threshold.  $t_c$  is the threshold of the ‘‘QCD continuum’’ that parametrizes, from the discontinuity of the Feynman diagrams, the spectral function  $\text{Im}\Pi_{\mathcal{H}}^{(1)}(t, m_c^2, \mu^2)$  where  $\Pi_{\mathcal{H}}^{(1)}(t, m_c^2, \mu^2)$  is the transverse scalar correlator corresponding to a spin one hadron:

$$\begin{aligned} \Pi_{\mathcal{H}}^{\mu\nu}(q^2) &= i \int d^4x e^{-iqx} \langle 0 | T \mathcal{O}_{\mathcal{H}}^\mu(x) (\mathcal{O}_{\mathcal{H}}^\nu(0))^\dagger | 0 \rangle, \\ &\equiv - \left( g^{\mu\nu} - \frac{q^\mu q^\nu}{q^2} \right) \Pi_{\mathcal{H}}^{(1)}(q^2) + \frac{q^\mu q^\nu}{q^2} \Pi_{\mathcal{H}}^{(0)}(q^2). \end{aligned} \quad (5)$$

### III. QCD TWO-POINT FUNCTION

Using the SVZ [25] OPE, we give in the Appendix the QCD expressions to LO of the two-point correlators associated to the currents given in Table I up to dimension  $d = 6$  condensate contributions.

#### A. LO PT and $1/N_c$ counting

Motivated by the criticisms raised in Ref. [47] based on the large  $N_c$  limit which state that the nonfactorized contribution of the two-point correlator starts at order  $\alpha_s^2$  and that the nonresonant (scattering states) dominate the sum rules, we check explicitly these statements for finite  $N_c$  here and in the following subsection C, which we complete in Sec. X by comparing the  $D^*D$  molecule resonance and the nonresonating  $D^*$  and  $D$  channels contributions to the sum rule.

The LO perturbative contributions are given by the diagrams in Fig. 2. Explicit evaluations of the trace appearing in the two-point function indicates that the LO PT contribution behaves like  $N_c^2$  [or  $2N_c^2(1 - 1/N_c)$  if the current has an  $\epsilon$  tensor like the one in Table I where the  $1/N_c$  term arises from the  $\epsilon$  contraction] as expected from large  $N_c$ .

However, nonfactorized contribution appears at LO both from PT and condensate contributions when one has two or more identical quark flavors because one has more possibilities to do the Wick’s contraction.<sup>5</sup> Moreover, some care has to be taken when applying the large  $N_c$  analysis to the case of baryons and tetraquark states with string junctions [3].

#### B. The LO $d \leq 6$ condensates contributions

The QCD condensates entering in the analysis are the light quark condensate  $\langle \bar{q}q \rangle$  and the  $SU(3)$ -breaking parameter  $\kappa \equiv \langle \bar{s}s \rangle / \langle \bar{q}q \rangle$ , the gluon condensates  $\langle \alpha_s G^2 \rangle \equiv \langle \alpha_s G_{\mu\nu}^a G_{\mu\nu}^a \rangle$  and  $\langle g^3 G^3 \rangle \equiv \langle g^3 f_{abc} G_{\mu\nu}^a G_{\nu\rho}^b G_{\rho\mu}^c \rangle$ , the mixed quark-gluon condensate  $g \langle \bar{q}Gq \rangle \equiv \langle \bar{q} g \sigma^{\mu\nu} (\lambda_a/2) G_{\mu\nu}^a q \rangle = M_0^2 \langle \bar{q}q \rangle$  and the four-quark condensate  $\rho \langle \bar{q}q \rangle^2$ , where

<sup>5</sup>Eye diagram of the type in Fig. 3 will not contribute in our analysis as it leads to nonopen charm final states.

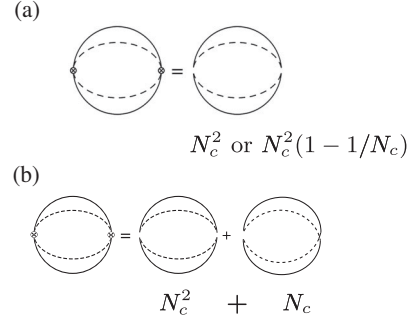


FIG. 2. LO PT contributions to the spectral function: (a) factorized, (b) factorized  $\oplus$  nonfactorized.



FIG. 3. LO eye diagram.

$\rho \simeq (3 \sim 4)$  indicates the deviation from the four-quark vacuum saturation. Their different contributions within the SVZ expansion to LO are shown in Figs. 4 to 8.

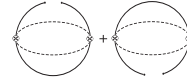


FIG. 4.  $\langle \bar{q}q \rangle$  quark condensate.

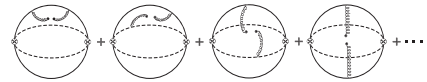


FIG. 5.  $\langle \alpha_s G^2 \rangle$  gluon condensate.

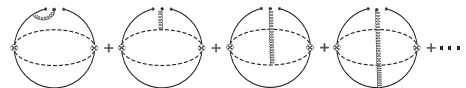


FIG. 6.  $g \langle \bar{q}Gq \rangle$  mixed quark-gluon condensate.

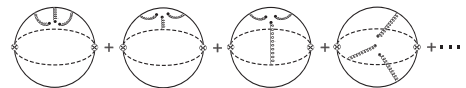


FIG. 7.  $\langle g^3 G^3 \rangle$  triple gluon condensate.



FIG. 8.  $\rho \langle \bar{\psi}\psi \rangle^2$  four-quark condensate.

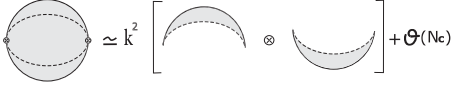


FIG. 9. The four-quark spectral function as a convolution of two quark bilinear ones [see Eq. (8)]. The black region means perturbative  $\oplus$  nonperturbative contributions.

Unlike often used in the literature, we have not included higher dimension  $d \geq 8$  condensates contributions<sup>6</sup> due to our poor knowledge of their size. Indeed, a violation of the vacuum saturation for the four-quark condensates [48–52] has been already noticed in different light quark channels. In addition, the mixing of different four-quark condensates under renormalization [46] does not also favor the vacuum saturation estimate. On the other, the inaccuracy of a simple dilute gas instanton estimate [25,53] has been also observed from the phenomenological estimate of high-dimension gluon condensates [54–56].

### C. Convolution representation and matching

We have explicitly proven in our previous papers [22–24,42,44] that the nonfactorized contribution to the four-quark correlator, which appears at lowest order  $\alpha_s^0$  of PT QCD to order in  $1/N_c$  (but not to order  $\alpha_s^2$  as claimed by [47]), gives numerically negligible contribution to the sum rule. Therefore, we can consider that the molecule/tetraquark two-point spectral function is well approximated by the convolution of the two ones built from two quark bilinear currents (factorization) as illustrated in Fig. 9 where the diagrams in the two sides of Fig. 9 are of the order  $N_c^2$ .

In order to fix the matching factor  $k^2$ , we consider the example of the  $D^*D$  molecule current where the QCD expression is given in the Appendix. The bilinear currents and the corresponding spectral functions entering in the RHS of Fig. 9 are

$$\begin{aligned} J^{P,S}(x) &\equiv \bar{c}[\gamma_5, 1]c \rightarrow \frac{1}{\pi} \text{Im}\psi^{P,S}(t) \sim \frac{3}{8\pi^2}, \\ J^{V,A}(x) &\equiv \bar{c}[\gamma_\mu, \gamma_\mu\gamma_5]c \rightarrow \frac{1}{\pi} \text{Im}\psi^{V,A}(t) \sim \frac{1}{4\pi^2}, \end{aligned} \quad (6)$$

in the limit where  $m_c^2 \ll t$ . In this way, we obtain, for a spin 1 state, the convolution integral [57–59]:

$$\begin{aligned} \frac{1}{\pi} \text{Im}\Pi_{\mathcal{H}}(t) &= \theta[t - (\sqrt{t_{10}} + \sqrt{t_{20}})^2] \left(\frac{k}{4\pi}\right)^2 t^2 \int_{t_{10}}^{(\sqrt{t}-\sqrt{t_{20}})^2} dt_1 \\ &\times \int_{t_{20}}^{(\sqrt{t}-\sqrt{t_1})^2} dt_2 2\lambda^{3/2} \left(\frac{t_1}{t}, \frac{t_2}{t}\right) \frac{1}{\pi} \text{Im}\psi^{S,P}(t_1) \\ &\times \frac{1}{\pi} \text{Im}\psi^{A,V}(t_2), \end{aligned} \quad (7)$$

<sup>6</sup>Some classes of  $d = 8$  contributions are given in [23,24].

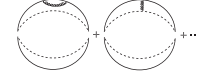


FIG. 10. NLO factorized PT contribution to the spectral function.

with the phase space factor:

$$\lambda\left(\frac{t_1}{t}, \frac{t_2}{t}\right) = \left(1 - \frac{(\sqrt{t_1} - \sqrt{t_2})^2}{t}\right) \left(1 - \frac{(\sqrt{t_1} + \sqrt{t_2})^2}{t}\right). \quad (8)$$

$\sqrt{t_{10}}$  and  $\sqrt{t_{20}}$  are the quark/hadronic thresholds and  $m_c$  is the on shell/pole perturbative charm quark mass.

The appropriate  $k$  factor that matches this convolution representation with the direct perturbative calculation of the molecule spectral function given in the Appendix is<sup>7</sup>

$$k^2 = \frac{5}{3 \times 2^6}, \quad (9)$$

which comes from the dynamics of the Feynman diagram calculations and which is missed in a standard large  $N_c$  results of [60]. Related phenomenology will be discussed in Sec. X.

### D. NLO PT corrections to the spectral functions

We extract the next-to-leading (NLO) PT corrections by approximating the molecule/tetraquark two-point spectral function with the convolution of the two ones built from two quark bilinear currents (factorization) illustrated in Fig. 10.

The NLO perturbative expressions of the bilinear unequal masses (pseudo)scalar and (axial)-vector spectral functions are known in the literature [27,28,31,61–63].

### E. From the on shell to the $\overline{\text{MS}}$ scheme

We transform the pole mass  $m_c$  to the running mass  $\bar{m}_c(\mu)$  using the known relation in the  $\overline{\text{MS}}$  scheme to order  $\alpha_s$  [27,28]

$$m_c = \bar{m}_c(\mu) \left[ 1 + \frac{4}{3} a_s + a_s \ln \frac{\mu^2}{m_c^2} + \mathcal{O}(a_s^2) \right].$$

In the following, we shall use  $n_f = 4$  total number of flavors for the numerical value of  $a_s \equiv \alpha_s/\pi$ .

## IV. QCD INPUT PARAMETERS

### A. QCD coupling $\alpha_s$

We shall use from the  $M_{\chi_{0c}} - M_{\eta_c}$  mass-splitting sum rule [64]:

<sup>7</sup>For the tetraquark case, one should add a factor (4/3).



TABLE II. QCD input parameters estimated from QSSR (moments, LSR, and ratios of sum rules) used here.

Parameters	Values	Sources	Ref.
$\alpha_s(M_Z)$	0.1181(16)(3)	$M_{\chi_{0c,b}} - M_{\eta_{c,b}}$	[64,66,67]
$\bar{m}_c(m_c)$ [MeV]	1266(6)	$D, B_c \oplus J/\psi, \chi_{c1}, \eta_c$	[64,67–69]
$\hat{\mu}_q$ [MeV]	253(6)	Light	[27,70]
$\hat{m}_s$ [MeV]	114(6)	Light	[27,70]
$\kappa \equiv \langle \bar{s}s \rangle / \langle \bar{d}d \rangle$	0.74(6)	Light-Heavy	[27,70,71]
$M_0^2$ [GeV <sup>2</sup> ]	0.8(2)	Light-Heavy	[27,36,51] [52,72–74]
$\langle \alpha_s G^2 \rangle$ [GeV <sup>4</sup> ]	$6.35(35)10^{-2}$	Light-Heavy	[64,67]
$\langle g^3 G^3 \rangle / \langle \alpha_s G^2 \rangle$	$8.2(1.0)[\text{GeV}^2]$	$J/\psi$	[54–56]
$\rho \alpha_s \langle \bar{q}q \rangle^2$ [GeV <sup>6</sup> ]	$5.8(9)10^{-4}$	Light, $\tau$ decay	[36,48–52]

$$\alpha_s(2.85) = 0.262(9) \rightarrow \alpha_s(M_\tau) = 0.318(15) \rightarrow \alpha_s(M_Z) = 0.1183(19)(3), \quad (10)$$

which is more precise than the one from  $M_{\chi_{0b}} - M_{\eta_b}$  [64]:

$$\alpha_s(9.50) = 0.180(8) \rightarrow \alpha_s(M_\tau) = 0.312(27) \rightarrow \alpha_s(M_Z) = 0.1175(32)(3). \quad (11)$$

These lead to the mean value quoted in Table II, which is in complete agreement with the world average [65]:

$$\alpha_s(M_Z) = 0.1181(11). \quad (12)$$

### B. Quark masses

We shall use the recent determinations of the running masses  $\bar{m}_s(\mu)$  and  $\bar{m}_c(\bar{m}_c)$  quoted in Table II and the corresponding value of  $\alpha_s$  evaluated at the scale  $\mu$  obtained using the same sum rule approach.

### C. QCD condensates

Their values are quoted in Table II. One should notice that taking into account the anomalous dimension of the  $\langle \bar{q}q \rangle$  condensate,  $\alpha_s \langle \bar{q}q \rangle^2$  has a very smooth  $1/\log(\tau\Lambda^2)^{1/25}$  behavior for  $n_f = 4$  flavors such that, contrary to simple minded, its contribution is not suppressed by  $1/\log(\tau\Lambda^2)$  for light mesons [48,49] and  $\tau$  decays [50] permitting its reliable phenomenological estimate while its extraction from light baryons [36,51,52] occurs without the  $\alpha_s$  factor like in the case of the four-quark currents discussed here.

## V. THE SPECTRAL FUNCTION

### A. The minimal duality ansatz

In the present case, with no complete data on the spectral function, we use the minimal duality ansatz:

$$\frac{1}{\pi} \text{Im}\Pi_{\mathcal{H}} \simeq f_{\mathcal{H}}^2 M_{\mathcal{H}}^8 \delta(t - M_{\mathcal{H}}^2) + \Theta(t - t_c) \frac{1}{\pi} \text{Im}\Pi_{\mathcal{H}}^{\text{QCD}}(t), \quad (13)$$

for parametrizing the molecule spectral function.  $M_{\mathcal{H}}$  and  $f_{\mathcal{H}}$  are the lowest ground state mass and coupling analog to  $f_\pi$ . The ‘‘QCD continuum’’ is the imaginary part of the QCD correlator [as mentioned after Eq. (4)] from the threshold  $t_c$ , which is assumed to smear all higher states contribution. Then, it ensures that both sides of the sum rules have the same large  $t$  asymptotic behavior that leads to the finite energy sum rule in Eq. (4). Within a such parametrization, one obtains

$$\mathcal{R}_n^c \equiv \mathcal{R} \simeq M_{\mathcal{H}}^2, \quad (14)$$

indicating that the ratio of moments is a useful tool for extracting the mass of the hadron ground state [27–29]. The corresponding value of  $t_c$  approximately corresponds to the mass of the first radial excitation. However, one should bear in mind that a such parametrization cannot distinguish two nearby resonances but instead will consider them as one ‘‘effective resonance.’’

This simple model has been tested successfully in different channels where complete data are available (charmonium, bottomium, and  $e^+e^- \rightarrow I = 1$  hadrons) [27,28,33]. It was shown that, within the model, the sum rule reproduces quite well the integrated data while the masses of the lowest ground state mesons ( $J/\psi$ ,  $\Upsilon$ , and  $\rho$ ) have been predicted within a good accuracy.

In the extreme case of the pseudoscalar Goldstone pion, the sum rule using the spectral function parametrized by this simple model and the more complete one by Chiral Perturbation Theory (ChPT) [75] lead to similar values of the sum of light quark masses ( $m_u + m_d$ ) indicating the efficiency of this simple parametrization [27,28].

An eventual violation of the quark-hadron duality (DV) [76,77] tested from hadronic  $\tau$ -decay data [50,77,78] is negligible here thanks to the double exponential suppression of this contribution in the Laplace sum rule (see, e.g., [42] for details).

The uses of this model for the tetraquarks and molecule states are also quite successful compared to the recent data (see, e.g., [42,44] and references therein). Then, we (*a priori*) expect to extract with a good accuracy the masses and couplings of the mesons within the approach.

In order to minimize the effects of radial excitations smeared by the QCD continuum, we shall work with the lowest moment  $\mathcal{L}_0^c$  and ratio of moments  $\mathcal{R}_0^c$  for extracting the meson masses and couplings  $f_{\mathcal{H}}$ . Moments with  $n < 0$  will not be considered due to their sensitivity on the nonperturbative contributions at zero momentum.

However, once we have fixed the ground state parameters, we attempt to extract the mass and coupling of the first radial excitation by using a ‘‘two resonance’’

+ $\Theta(t - t_{c1})$  ‘‘QCD continuum’’ parametrization, where  $t_{c1}$  is above the  $t_c$  value obtained for the ground state.

### B. Optimization criteria

As  $\tau$ ,  $t_c$ , and  $\mu$  are free external parameters, we shall use stability criteria (minimum sensitivity on the variation of these parameters) to extract the hadron masses and couplings. Results based on these stability criteria have led to successful predictions in the current literature (see [27–29] and original papers).

## VI. REVISITING $f_{D^*D}$ AND $M_{D^*D}$

We start by revisiting and checking the results obtained in [24] where they have included the factorized contributions to the next-to-next-to leading order of perturbative series. In this example, we show explicitly our strategy for extracting the mass and coupling. The same strategy will be used in some other channels discussed later in this paper. This example is also a test of the efficiency of the method by confronting the prediction with the  $Z_c(3900)$  [79,80],  $Z_c(4020)$  [81],  $Z_c(4025)$  [82],  $Z_c(4050)$  [83],  $Z_c(4226)$ ,  $Z_c(4257)$  by BESIII [84], and  $Z_c(4430)$  [85,86] found earlier, where one can notice that only the  $Z_c(3900)$  and  $Z_c(4430)$  have been retained as established in the Meson summary table of Particle Data Group (PDG) [65].

### A. $\tau$ and $t_c$ stabilities

We show in Fig. 11 the  $\tau$  behavior of the coupling and of the mass for different values of  $t_c$  and fixing the value of the subtraction constant  $\mu$  at 4.65 GeV (see next subsection) where a  $\mu$  stability ( $4.5 \pm 0.5$ ) GeV has been found in [24]. From this figure, one can see that the coupling presents minimums in  $\tau$  and the mass inflexion points.

In a first step, we use the experimental mass  $M_{Z_c} = 3900$  MeV for extracting the value of the coupling  $f_{D^*D}$  shown in Fig. 11(a).

In a second step, we take the value of  $\tau$  at the minimum of the coupling and use it for extracting the value of  $M_{D^*D}$  from Fig. 11(b).

In a third step, we take the common range of  $t_c$  where both curves present stabilities in  $\tau$ . In the present case, this value ranges from  $t_c = 22$  GeV<sup>2</sup> (beginning of  $\tau$  stability) to  $t_c = 38$  GeV<sup>2</sup> (beginning of  $t_c$  stability) where the range is given in Table IV. For the mean  $t_c = 30$  GeV<sup>2</sup>, it is  $\tau_R \simeq 0.38$  (respectively, 0.34) GeV<sup>-2</sup> for LO (respectively, NLO) QCD expression.

The errors given in Table III and the resulting values of  $f_{D^*D}$  and  $M_{D^*D}$  in Table VII are the mean of the ones from the previous two extremal values of  $t_c$ .

### B. $\mu$ stability

For doing the analysis, we shall fix  $t_c = 30$  GeV<sup>2</sup>, which is the mean of the two extremal values delimiting the

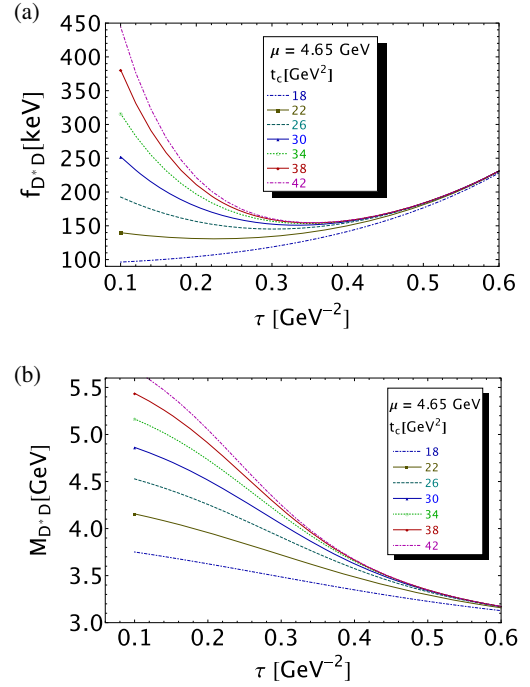


FIG. 11.  $f_{D^*D}$  and  $M_{D^*D}$  as function of  $\tau$  at NLO for different values of  $t_c$ , for  $\mu = 4.65$  GeV and for values of  $\bar{m}_c(\bar{m}_c)$  given in Table II.

stability region and take  $M_{D^*D} = 3900$  MeV for fixing the coupling. The analysis is shown in Fig. 12. One can see a  $\mu$  stability for

$$\mu = (4.65 \pm 0.05) \text{ GeV}, \quad (15)$$

at which we shall evaluate the results quoted in Table III.

This value of  $\mu$  from a more refined analysis is more precise than the conservative one ( $4.5 \pm 0.5$ ) GeV quoted in [24]. The results of the analysis are given in Tables III and VII.

One should note that the resummed QCD expression of the sum rule, which obeys an ‘‘homogeneous’’ renormalization group equation (RGE), is obtained by putting  $\mu^2 = 1/\tau$  in the QCD expression of the sum rule, and where the parameters having anomalous dimension  $\gamma$  run as  $1/(\log \tau \Lambda^2)^{\gamma/\beta}$  (see, e.g., [40]). We have often used this choice in the past (see [27–29]), which corresponds here to the value

$$\mu = 1/\sqrt{\tau_0} \simeq 1.6 \text{ GeV} \quad (16)$$

at the  $\tau$  minimum for  $t_c = 30$  GeV<sup>2</sup>. However, this value is outside the  $\mu$ -stability region obtained previously and then does not correspond to the optimal choice of  $\mu$ . This is the reason why we have abandoned this choice  $\mu^2 = 1/\tau$ . This result does not support the argument of Ref. [87] based on the observation that, when the term of the type  $(\alpha_s(\tau)/\alpha_s(\mu))^{\gamma/\beta_1}$  disappears for  $\mu = 1/\sqrt{\tau}$ , one would obtain the best choice of  $\mu$ . Indeed, the PT series behaves obviously much better in the

TABLE III. Sources of errors and predictions from LSR at NLO for the couplings and masses of the molecules and tetraquark ground states. The errors from the QCD input parameters are from Table II. We take  $|\Delta\tau| = 0.01 \text{ GeV}^{-2}$  and  $\Delta\mu = 0.05 \text{ GeV}$ . The quoted errors are the mean from the two extremal values of  $t_c$  delimiting the stability region quoted in Table IV.

Observables	$\Delta t_c$	$\Delta\tau$	$\Delta\mu$	$\Delta\alpha_s$	$\Delta PT$	$\Delta m_s$	$\Delta m_c$	$\Delta\bar{\psi}\psi$	$\Delta\kappa$	$\Delta G^2$	$\Delta M_0^2$	$\Delta\bar{\psi}\psi^2$	$\Delta G^3$	$\Delta OPE$	$\Delta M_G$	$\Delta f_G$	$\Delta M_{(G)_1}$	Values
<b>Coupling <math>f_G</math> [keV]</b>																		
<i>Molecule <math>(c\bar{d})(\bar{c}u)</math></i>																		
$D^*D$	11.0	0.10	0.50	2.10	0.03	...	1.25	1.90	...	0.0	1.15	5.60	0.0	6.20	3.12	...	...	140(15)
$D_0^*D_1$	9.80	0.20	0.14	0.80	17.0	...	0.70	4.30	...	0.14	1.60	7.60	0.06	7.30	2.08	...	...	96(23)
<i>Tetraquark <math>(\bar{c}\bar{d})(cu)</math></i>																		
$A_{cd}$	12.6	0.10	0.60	2.90	0.47	-	1.60	2.80	-	0.0	1.80	6.60	0.0	8.16	3.11	...	...	173(17)
<i>Molecule <math>(c\bar{s})(\bar{c}u)</math></i>																		
$D_s^*D$	12.4	0.10	0.50	2.40	0.07	0.0	2.0	1.90	3.20	0.0	0.90	4.30	0.0	4.80	1.93	...	...	130(15)
$D^*D_s$	12.2	0.10	0.50	2.40	0.11	0.07	1.40	1.70	3.20	0.02	1.30	4.40	0.03	7.0	2.19	...	...	133(16)
$D_{s0}^*D_1$	9.0	0.20	0.45	0.53	18.0	0.48	0.85	4.10	1.12	0.36	1.65	6.60	0.33	6.90	1.97	...	...	86(23)
$D_0^*D_{s1}$	8.60	0.20	0.15	0.86	17.5	0.20	0.75	3.60	1.60	0.02	1.80	6.50	0.07	6.90	1.95	...	...	89(22)
<i>Tetraquark <math>(\bar{c}\bar{s})(cu)</math></i>																		
$A_{cs}$	13.2	0.12	0.60	2.80	0.01	0.20	1.60	1.90	3.70	0.0	2.0	5.40	0.0	6.70	2.34	...	...	148(17)
<i>Molecule <math>(c\bar{s})(\bar{c}s)</math></i>																		
$D_s^*D_s$	9.60	0.11	0.40	2.40	1.40	0.10	1.30	2.0	5.90	0.0	1.10	3.50	0.05	2.40	3.35	...	...	114(13)
$D_{s0}^*D_{s1}$	9.60	0.20	0.13	0.80	5.90	0.41	0.75	4.35	1.73	0.05	1.58	5.50	0.08	3.50	2.31	...	...	79(14)
<i>Tetraquark <math>(\bar{c}\bar{s})(cs)</math></i>																		
$A_{css}$	10.9	0.14	0.50	2.80	0.90	0.25	1.40	2.10	6.90	0.0	2.0	4.40	0.10	5.20	2.40	...	...	114(15)
<b>Mass <math>M_G</math> [MeV]</b>																		
<i>Molecule <math>(c\bar{d})(\bar{c}u)</math></i>																		
$D^*D$	15.0	40.0	2.0	6.30	0.0	...	2.80	13.5	...	0.0	5.30	11.0	0.0	39.0	...	...	...	3912(61)
$D_0^*D_1$	1.60	105	4.50	9.50	2.50	...	7.10	50.0	...	1.80	12.0	40.0	0.30	39.5	...	...	...	4023(130)
<i>Tetraquark <math>(\bar{c}\bar{d})(cu)</math></i>																		
$A_{cd}$	8.30	38.0	1.90	7.50	1.90	...	2.90	10.0	...	0.06	4.90	7.10	0.0	39.5	...	...	...	3889(58)
<i>Molecule <math>(c\bar{s})(\bar{c}u)</math></i>																		
$D_s^*D$	5.70	37.8	2.50	7.50	0.23	2.50	3.0	8.0	15.0	0.0	7.0	10.0	0.0	25.4	...	...	...	3986(51)
$D^*D_s$	1.50	37.6	2.0	7.0	0.03	2.70	2.30	8.80	17.0	0.06	10.0	6.20	0.18	33.8	...	...	...	3979(56)
$D_{s0}^*D_1$	13.1	105	4.25	6.25	1.30	3.75	6.50	20.0	44.0	0.20	18.0	20.9	0.23	57.5	...	...	...	4064(133)
$D_0^*D_{s1}$	18.8	102	4.0	8.80	0.28	2.80	5.30	30.3	51.2	0.06	12.6	19.3	0.16	52.8	...	...	...	4070(133)
<i>tetraquark <math>(\bar{c}\bar{s})(cu)</math></i>																		
$A_{cs}$	8.50	38.8	2.0	6.90	0.03	2.20	2.40	7.60	16.0	0.07	7.50	6.70	0.0	33.5	...	...	...	3950(56)
<i>Molecule <math>(c\bar{s})(\bar{c}s)</math></i>																		
$D_s^*D_s$	0.30	42.5	2.40	6.0	12.0	6.20	2.10	6.70	15.3	0.05	9.10	13.8	0.05	25.7	...	...	...	4091(57)
$D_{s0}^*D_{s1}$	0.10	108	2.75	4.30	0.05	5.0	10.3	15.0	30.5	0.25	15.0	30.3	0.38	50.1	...	...	...	4198(129)
<i>Tetraquark <math>(\bar{c}\bar{s})(cs)</math></i>																		
$A_{css}$	1.60	44.0	15.0	15.0	0.06	16.0	13.0	23.0	16.0	0.15	12.3	17.0	0.08	43.7	...	...	...	4014(77)

$\mu$ -stability region where the value of  $\mu$  is about three times higher at which the radiative corrections are more suppressed.

Moreover, the physical meaning of the relation between  $\mu$  with the so-called bound energy or virtuality  $\mu^2 = M_Z^2 - 4M_c^2$  used in his different papers (see, e.g., [87,88]) remains unclear to us where  $M_c$  is the PT constituent or pole charm quark mass taken by the author to be about 1.84 GeV which corresponds to  $\mu \simeq 1.3 \text{ GeV}$ .

Indeed, one may expect from this formula that the difference between the resonance and PT quark constituent masses has a nonperturbative origin that (*a priori*) has nothing to do with the scale  $\mu$  where the PT series and the Wilson coefficients of the condensates are evaluated.

However, one may also consider  $\mu$  as a scale separating the calculable PT Wilson coefficients and the NPT noncalculable condensates in the OPE [25], though one has to bear in mind that the  $d \leq 6$  condensates appearing in the present analysis are renormalization group invariant ( $\mu$  independent like  $m_c \langle \bar{q}q \rangle$ ,  $m_c^2 \langle \bar{q}q \rangle^2$ ) or have a weak dependence on  $\mu$  ( $\langle \alpha_s G^2 \rangle$ ,  $\langle g\bar{q}Gq \rangle$ ) [27] (Part VII, page 285) such that the truncation of the PT series does not affect much their values. This feature indicates that the separation of the condensates from the PT Wilson coefficients are not ambiguous while the size of the nonperturbative condensate is almost independent on the scale at which the PT series is truncated.

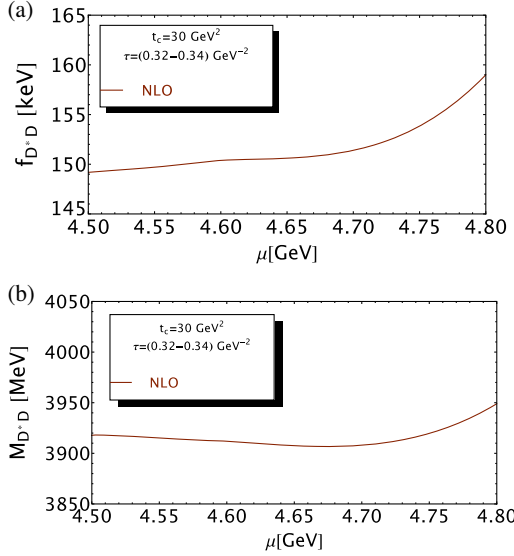


FIG. 12.  $f_{D^*D}$  and  $M_{D^*D}$  as function of  $\mu$  at NLO and for  $t_c = 30 \text{ GeV}^2$ .

### C. NLO and truncation of the perturbative series

We have mentioned in previous works that the inclusion of the NLO perturbative corrections is important for justifying the choice of heavy quark mass definition used in the analysis where an *ad hoc* value of the  $\overline{MS}$  running mass is frequently used in the literature while the spectral function has been evaluated using an on shell renormalization where the pole (on shell) quark mass naturally enters into the LO expression.

We show the analysis for the mass and coupling in Fig. 13 at fixed value of the continuum threshold  $t_c$  and subtraction constant  $\mu$ , where one can find that the use of the pole mass at LO decreases by 30% at the minimum (respectively, increases by 0.5% at the inflexion point) the value of the coupling (respectively, mass) obtained using the  $\overline{MS}$  running mass at LO while the NLO correction is relatively small within the  $\overline{MS}$  scheme.

The smallness of radiative corrections for the ratio of moments demonstrates (*a posteriori*) why the use of the  $\overline{MS}$  running mass at LO leads to a surprisingly good prediction for the mass.

Assuming that the PT series grow geometrically [89–92], one can deduce from the previous analysis an estimate of higher order PT contributions given in Table III which can be compared with the ones in [23,24].

### D. QCD condensates and truncation of the OPE

We show in Fig. 14 the contributions of the QCD condensates for different truncations of the OPE. Fixing  $\tau \approx 0.34 \text{ GeV}^{-2}$ , where the final value of the coupling presents  $\tau$  stability and the mass inflexion points, one obtains for  $t_c = 30 \text{ GeV}^2$ :

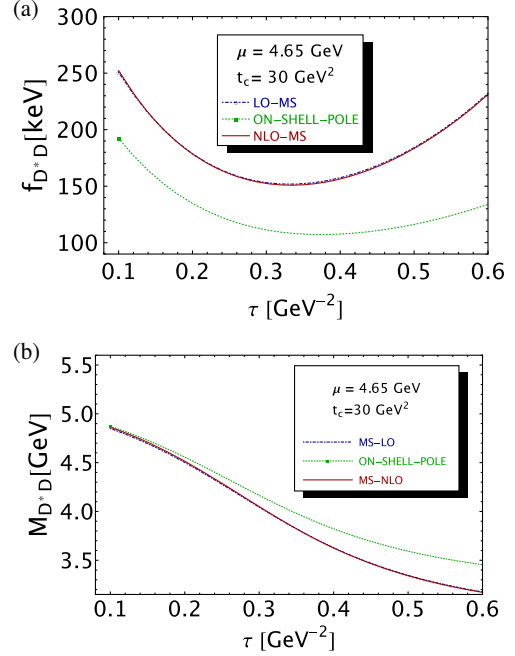


FIG. 13.  $f_{D^*D}$  and  $M_{D^*D}$  as function of  $\tau$  at LO and NLO for  $t_c = 30 \text{ GeV}^2$  and  $\mu = 4.65 \text{ GeV}$  for different definitions of the charm quark mass. We use  $m_c(\text{pole}) = 1.5 \text{ GeV}$  and the running mass given in Table II.

$$f_{D^*D} \simeq 56 \text{ keV}[1 + 0.98 - 0.13 + 0.86] \\ \simeq 151 \text{ keV},$$

$$M_{D^*D} \simeq 4683 \text{ MeV}[1 - 0.08 + 0.02 - 0.12] \\ \simeq 3864 \text{ MeV}. \quad (17)$$

One can notice the important role of the dimension-4 and -6 condensates that are dominated by the chiral condensates  $\langle \bar{q}q \rangle$  and  $\rho \langle \bar{q}q \rangle^2$  in the extraction of the coupling and mass where their strengths are more pronounced for the coupling.

We estimate the systematic errors due to the truncation of the OPE from the size of the dimension-6 condensate contributions rescaled by the factor  $m_c^2 \tau / 3$  where 1/3 comes from the LSR exponential form of the sum rule. It can be compared with the contributions of the known  $d = 8 \langle \bar{q}q \rangle \langle \bar{q}Gq \rangle$  condensate obtained in [23,24] but bearing in mind that this is only a part of the complete  $d = 8$  condensate ones where the validity of the vacuum saturation used for its estimate is questionable.

The quoted errors in Table III are the mean from the two extremal values of  $t_c$  delimiting the  $(\tau, t_c)$  stability region. We expect that the systematics for the  $m_s \neq 0$  cases are similar as confirmed explicitly in Table III.

### E. Vacuum saturation of the four-quark condensate

The four-quark condensates have been demonstrated to mix under renormalization [27,46] (Part VII, page 285) at finite  $N_c$  while its vacuum saturation estimate is only valid



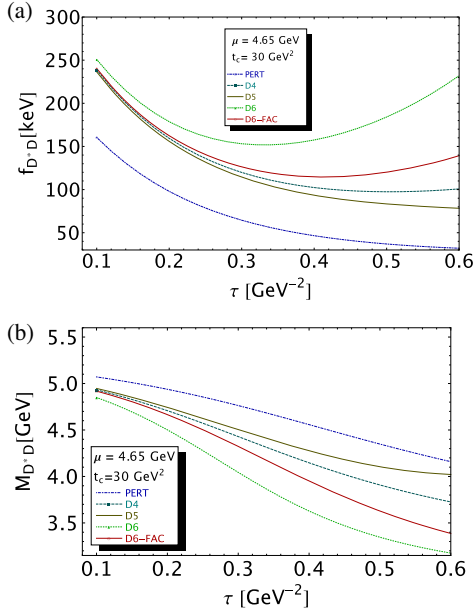


FIG. 14.  $f_{D^*D}$  and  $M_{D^*D}$  as function of  $\tau$  at NLO for  $t_c = 30 \text{ GeV}^2$  and  $\mu = 4.65 \text{ GeV}$  and for different truncations of the OPE.  $D4 \equiv$  perturbative  $\oplus$  dimension 4;  $D5 \equiv D4 \oplus$  dimension 5;  $D6 \equiv D5 \oplus$  dimension 6. The values of  $\bar{m}_c(\bar{m}_c)$  and the condensates are given in Table II. FAC means that we use the vacuum saturation assumption for the estimate of the four-quark condensates.

in the large  $N_c$  limit. A such estimate from light mesons [48,49], light baryons [36,51,52], and  $\tau$  decays [50] has been shown to underestimate the actual value of the four-quark condensates by a factor of 3–4 (see also the comments in Sec. IV C). For completeness, we also show in Fig. 14 the effect of this estimate, where we see that the position of the minimum and inflexion point are shifted at  $\tau \approx 0.4 \text{ GeV}^{-2}$ . At this value and for  $t_c = 30 \text{ GeV}^2$ , one obtains an effect of +38% for the coupling and -7% for the mass leading to

$$f_{D^*D}|_{FAC} \approx 115 \text{ keV}, \quad M_{D^*D}|_{FAC} \approx 3951 \text{ MeV}, \quad (18)$$

which can be compared with the one in Eq. (17).

### F. Results of the analysis

The sizes of the errors from different sources and the final results are collected in Tables III and VII:

$$f_{D^*D} = 140(15) \text{ keV}, \quad M_{D^*D} = 3912(61) \text{ MeV}. \quad (19)$$

One can notice that the results are in perfect agreement with the previous ones in [24]. The slight difference in the error calculation is due to the fact that, in Ref. [24], we have estimated the error by choosing  $t_c = 38 \text{ GeV}^2$  but not considering the one due to  $t_c = 22 \text{ GeV}^2$ .

The result for the mass is in a very good agreement with the BELLE [79] and BESIII [80] data  $Z_c(3900) \text{ MeV}$ , which we shall discuss later on.

## VII. REVISITING $f_{D_0^*D_1, A_{cd}}$ AND $M_{D_0^*D_1, A_{cd}}$

Here, we also revisit the estimate of the  $D_0^*D_1, A_{cd}$  masses and couplings done in [24]. We repeat exactly the same procedure as in the previous section.

### A. $f_{D_0^*D_1}$ and $M_{D_0^*D_1}$

The  $\tau$  and  $t_c$  behaviors of the coupling and mass are similar to the previous case and will not be shown here. The  $\tau$ -stability region ranges from  $\tau = 0.21 \text{ GeV}^{-2}$  for  $t_c = 28 \text{ GeV}^2$  (beginning of  $\tau$  stability) to  $0.30 \text{ GeV}^{-2}$  for  $t_c = 40 \text{ GeV}^2$  (beginning of  $t_c$  stability). One can notice that the  $\tau$  stability starts at a larger value of  $t_c$  than the one  $t_c = 22 \text{ GeV}^2$  for the case of  $D^*D$  which will imply a larger value of  $M_{D_0^*D_1}$  than of  $M_{D^*D}$ .

The  $\mu$  stability is shown in Fig. 15 where the optimal value is the same as in Eq. (15). The result,

$$f_{D_0^*D_1} = 96(23) \text{ keV}, \quad M_{D_0^*D_1} = 4023(130) \text{ MeV}, \quad (20)$$

differs with the one given in [23,24] (see Table VII), which was originated from the unprecise value of the  $\tau$  used there for extracting the optimal value, which affects in a sensible way the value of the mass in this channel.

### B. $f_{A_{cd}}$ and $M_{A_{cd}}$

The  $\tau$  and  $t_c$  behaviors of the  $A_{cd}$  mass and coupling are similar to the one in Fig. 11. The  $\tau$  stability starts for  $t_c = 22 \text{ GeV}^2$  at  $\tau = 0.25 \text{ GeV}^{-2}$  while the  $t_c$  stability starts at  $t_c = 38 \text{ GeV}^2$  where  $\tau = 0.36 \text{ GeV}^{-2}$ .

The  $\mu$  behaviors are the same as the ones of  $D_0^*D_1$  where the  $\mu$  stability is also at  $4.65 \text{ GeV}$  as in Eq. (15).

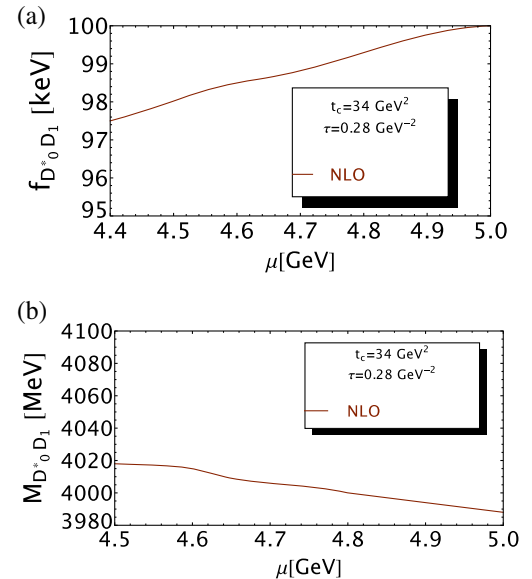


FIG. 15.  $f_{D_0^*D_1}$  and  $M_{D_0^*D_1}$  as function of  $\mu$  at NLO and for  $t_c = 30 \text{ GeV}^2$ .

TABLE IV. Values of the set of the LSR parameters ( $t_c, \tau$ ) at the optimization region for the PT series up to NLO and for the OPE truncated at the dimension-six condensates and for  $\mu = 4.65$  GeV.

States	$(1^+)$ ground states										
	$D^*D$	$D_s^*D$	$D^*D_s$	$D_s^*D_s$	$D_0^*D_1$	$D_{s0}^*D_1$	$D_0^*D_{s1}$	$D_{s0}^*D_{s1}$	$A_{cd}$	$A_{cs}$	$A_{css}$
$t_c$ [GeV <sup>2</sup> ]	22–38	22–38	22–38	24–40	28–40	28–44	28–44	28–44	22–38	22–8	24–40
$\tau$ [GeV] <sup>-2</sup> 10 <sup>2</sup>	23; 35	22; 36	24; 38	24; 36	21; 30	20; 30	23; 31	20; 30	25; 37	25; 38	27; 38

The estimates of the errors and the results for the coupling and mass

$$f_{A_{cd}} = 173(17) \text{ keV}, \quad M_{A_{cd}} = 3889(58) \text{ MeV} \quad (21)$$

are collected in Tables III and VII. The mass value is in good agreement with the one 3888(130) MeV obtained in Ref. [24] but with a smaller error due to a better localization of the  $\tau$  and  $\mu$  stability points. The  $A_{cd}$  mass also coincides with the observed  $Z_c(3900)$ . The different sets of ( $t_c, \tau$ ) used to get the previous optimal results are summarized in Table IV.

### VIII. THE $(1^+)$ $(c\bar{s})(\bar{c}u)$ AND $(\bar{c}\bar{s})(cu)$ STATES

#### A. New estimate of $f_{D_s^*D}$ and $M_{D_s^*D}$

In this section, we present a new estimate of the  $D_s^*D$  molecule mass and coupling.

The  $\tau$  and  $t_c$  behaviors of the coupling and mass are also similar to the previous cases as shown in Fig. 16.

The  $\tau$ -stability region ranges from  $\tau = 0.22$  GeV<sup>-2</sup> for  $t_c = 22$  GeV<sup>2</sup> (beginning of  $\tau$  stability) until 0.36 GeV<sup>-2</sup> for 38 GeV<sup>2</sup> (beginning of  $t_c$  stability).

The  $\mu$  stability is shown in Fig. 17 where the optimal value is the same as in Eq. (15).

The sources of the errors and the results are quoted in Tables III and VII. One can notice that the values of the  $\tau$ ,  $t_c$ , and  $\mu$  stabilities are about the same as in the case of  $D^*D$  indicating a good  $SU(3)$  symmetry for the sum rule parameters. The obtained values quoted in Tables III and VII :

$$f_{D_s^*D} = 130(15) \text{ keV}, \quad M_{D_s^*D} = 3986(51) \text{ MeV} \quad (22)$$

also indicate small  $SU(3)$  breakings of chiral symmetry, which is about  $-7.1\%$  for the coupling and  $+1.9\%$  for the mass.

#### B. New estimate of $f_{D^*D_s}$ and $M_{D^*D_s}$

A similar analysis is done for extracting  $f_{D^*D_s}$  and  $M_{D^*D_s}$ . The  $\tau$  and  $t_c$  behaviors of the results are similar to the previous ones. The  $\mu$  behavior is shown in Fig. 18. We obtain

$$f_{D^*D_s} = 133(16) \text{ keV}, \quad M_{D^*D_s} = 3979(56) \text{ MeV}, \quad (23)$$

where the values of the parameters are about the same as the ones of  $D_s^*D$  as intuitively expected. They are quoted in Tables III and VII.

#### C. The $D_{s0}^*D_1$ and $D_0^*D_{s1}$ molecules

Similar analysis leads to (see Tables III and VII):

$$\begin{aligned} f_{D_{s0}^*D_1} &= 86(23) \text{ keV}, & M_{D_{s0}^*D_1} &= 4064(133) \text{ MeV}, \\ f_{D_0^*D_{s1}} &= 89(23) \text{ keV}, & M_{D_0^*D_{s1}} &= 4070(133) \text{ MeV}, \end{aligned} \quad (24)$$

where one can notice that the two molecule states are almost degenerated and have the same couplings to the currents.

#### D. The $A_{cs}$ tetraquark

We pursue the previous analysis for the  $A_{cs}$  tetraquark. The behaviors of the different curves are similar to the previous ones and will not be shown. The result quoted in Tables III and VII is

$$f_{A_{cs}} = 148(17) \text{ keV}, \quad M_{A_{cs}} = 3950(56) \text{ MeV}, \quad (25)$$

where one can notice that it is almost degenerated to the  $D^*D_s$  and  $D_s^*D$  and has almost the same couplings.

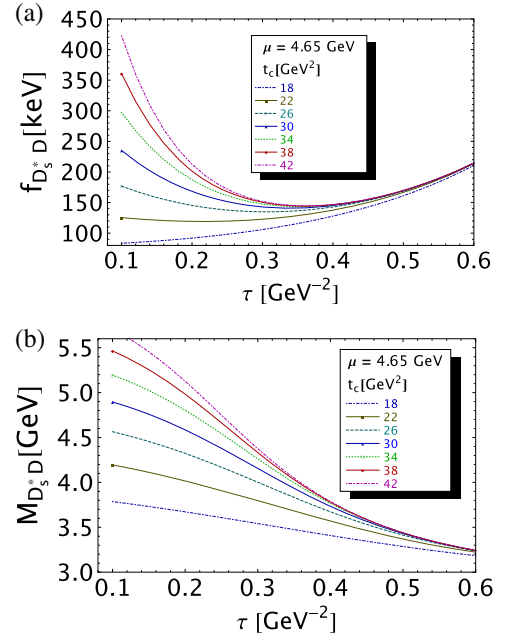


FIG. 16.  $f_{D_s^*D}$  and  $M_{D_s^*D}$  as function of  $\tau$  at NLO for different values of  $t_c$ , for  $\mu = 4.65$  GeV and for values of  $\bar{m}_c(\bar{m}_c)$  given in Table II.

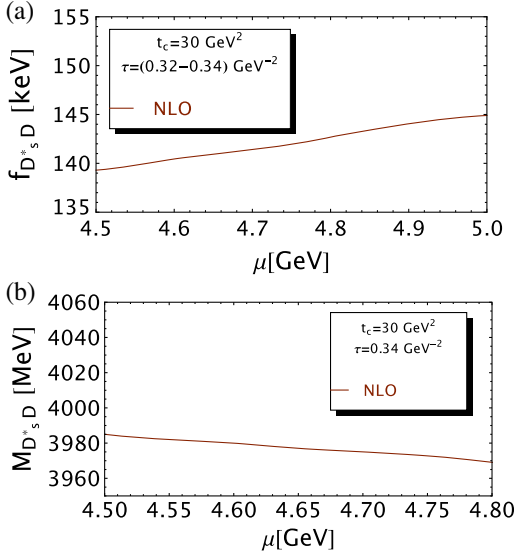


FIG. 17.  $f_{D_s^* D_s}$  and  $M_{D_s^* D_s}$  as function of  $\mu$  at NLO and for  $t_c = 30 \text{ GeV}^2$ .

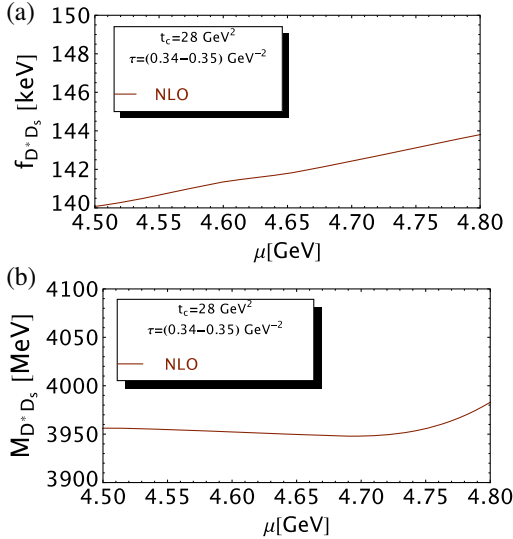


FIG. 18.  $f_{D_s^* D_s}$  and  $M_{D_s^* D_s}$  as function of  $\mu$  at NLO and for  $t_c = 28 \text{ GeV}^2$ .

### IX. THE $(1^+)$ $(c\bar{s})(\bar{c}s)$ AND $(\bar{c}\bar{s})(cs)$ STATES

In this section, we revisit and improve our previous estimate of the masses and couplings of these aforementioned states and give a new estimate of the  $D_s^* D_s$  radial excitation mass and coupling.

#### A. The $D_s^* D_s$ molecule

The analysis of the  $\tau$  and  $t_c$  behaviors is shown in Fig. 19. The  $\mu$  behavior is shown in Fig. 20. These behaviors are similar to the previous ones. The  $(\tau, t_c)$  stabilities are obtained for  $t_c$  inside the range 24 to 40  $\text{GeV}^2$ . We deduce (see Tables III and VII):

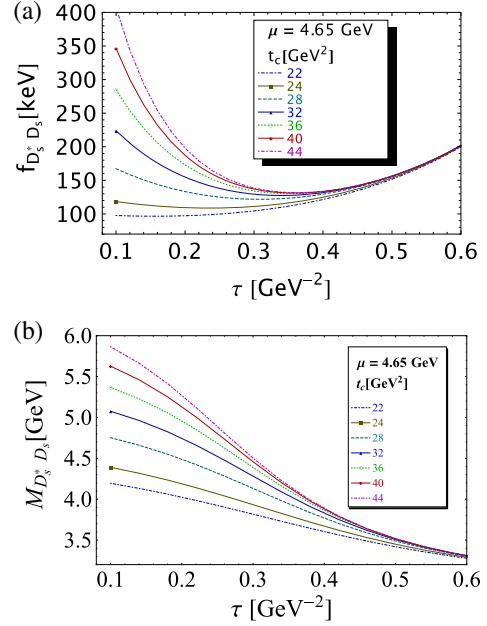


FIG. 19.  $f_{D_s^* D_s}$  and  $M_{D_s^* D_s}$  as function of  $\tau$  at NLO for different values of  $t_c$ , for  $\mu = 4.65 \text{ GeV}$  and for values of  $\bar{m}_c(\bar{m}_c)$  given in Table II.

$$f_{D_s^* D_s} = 114(13) \text{ keV}, \quad M_{D_s^* D_s} = 4091(57) \text{ MeV}. \quad (26)$$

One can notice the (almost) similar effect of  $SU(3)$  breakings than in the previous cases. The mass increases by 105 MeV compared to the one of the  $D_s^* D$  state which is about the one 74 MeV from  $D^* D$  to  $D_s^* D$ .

#### B. The $D_{s0}^* D_{s1}$ molecule and $A_{css}$ tetraquark

In this section, we revise and check the results obtained in [23]. The behaviors of the  $\tau$ ,  $t_c$ , and  $\mu$  behaviors of the

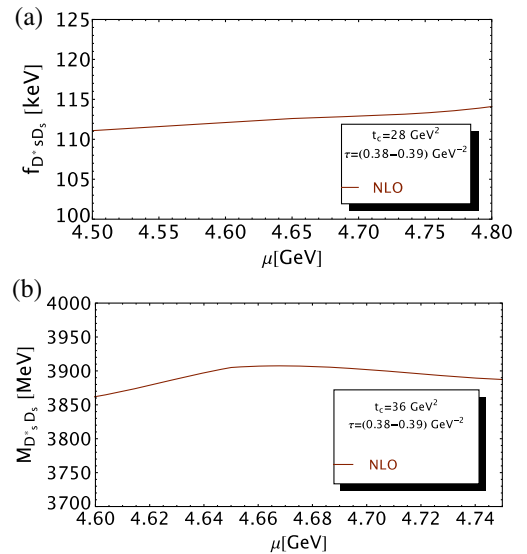


FIG. 20.  $f_{D_s^* D_s}$  and  $M_{D_s^* D_s}$  as function of  $\mu$  at NLO and for  $t_c = 36 \text{ GeV}^2$ .

masses and couplings are similar to the previous cases and will not be shown.

For the  $D_{s0}^*D_{s1}$  molecule, the set of  $(\tau, t_c)$  stabilities are obtained from (0.20,28) to (0.30,44) in units of  $(\text{GeV}^{-2}, \text{GeV}^2)$ , where one notice the sensitivity of the results in the change of  $\tau$ , which is quantified by the large error induced by the variation of  $\tau$  as shown in Table III. One obtains from Tables III and VII

$$f_{D_{s0}^*D_{s1}} = 79(14) \text{ keV}, \quad M_{D_{s0}^*D_{s1}} = 4198(129) \text{ MeV}, \quad (27)$$

which agree within the errors with the previous results in [23].

For the  $A_{css}$  tetraquark,  $\tau$  stability at  $0.27 \text{ GeV}^{-2}$  starts for  $t_c = 24 \text{ GeV}^2$  while the  $t_c$  stability for  $\tau = 0.38 \text{ GeV}^{-2}$  starts for  $t_c = 40 \text{ GeV}^2$ . These values are about the same as the ones for  $A_{cd}$  and  $A_{cs}$  indicating like in the case of molecule states a good  $SU(3)$  symmetry for the values of the LSR parameters. The optimal results are given in Tables III and VII, which read

$$f_{A_{css}} = 114(16) \text{ keV}, \quad M_{A_{css}} = 4014(86) \text{ MeV}. \quad (28)$$

Compared to the previous nonstrange case where the molecule  $D^*D$  is quasidegenerated with the tetraquark  $A_{cd}$ , which leads us to conclude that the observed state is a tetramole  $\mathcal{T}_c$ , in this channel, we find the tetraquark  $A_{css}$  is almost degenerated (within the errors) with the molecule  $D_s^*D_s$  and has the same couplings implying that it can also be a tetramole  $\mathcal{T}_{css}$  state with a coupling and mass:

$$f_{\mathcal{T}_{css}} = 114(10) \text{ keV}, \quad M_{\mathcal{T}_{css}} = 4064(46) \text{ MeV}. \quad (29)$$

The  $D_{s0}^*D_{s1}$  molecule is about  $100 \text{ MeV}$  slightly higher but has a weaker coupling to the corresponding current.

## X. TWO-MESON SCATTERING STATES

To study this contribution, we take the example of the  $D^*D$  molecule.<sup>8</sup>

We saturate the rhs of Fig. 9 by the two nonresonant (scattering) states  $D^*$  and  $D$ , which we shall compare with the one due to the molecule  $D^*D$  (lhs) appropriately matched with the  $k^2$  factor.

Then, one obtains the two-resonance scattering LSR moment:

$$\begin{aligned} \mathcal{L}_0^c(D^* \oplus D) &\equiv 2 \left( \frac{k}{4\pi} \right)^2 f_{D^*}^2 \left( \frac{f_D}{m_c} \right)^2 \mathcal{I}(t, M_D^2, M_{D^*}^2) \\ &\simeq 1.16 \times 10^{-6} \text{ GeV}^{10}, \end{aligned} \quad (30)$$

<sup>8</sup>Our conclusion remains valid for some other molecules and tetraquarks states.

where  $\mathcal{I}(t, M_D^2, M_{D^*}^2)$  is the integral [see Eq. (6)]:

$$\begin{aligned} \mathcal{I} &\equiv \int_{(M_D+M_{D^*})^2}^{t_c} dt t^2 e^{-t\tau} \int_{M_D^2}^{(\sqrt{t}-M_{D^*})^2} dt_1 \\ &\times \int_{M_{D^*}^2}^{(\sqrt{t}-\sqrt{t_1})^2} dt_2 \lambda^{3/2} \left( \frac{M_D^2}{t}, \frac{M_{D^*}^2}{t} \right), \end{aligned} \quad (31)$$

to be compared with the molecule sum rule result:

$$\mathcal{L}_0^c(D^*D) \equiv f_{D^*D}^2 M_{D^*D}^8 e^{-\tau_R M_{D^*D}^2} \simeq 1.09 \times 10^{-5} \text{ GeV}^{10}, \quad (32)$$

which we have evaluated at the stability point  $\tau_R \simeq 0.3 \text{ GeV}^{-2}$ . We have used the previous values of the molecule parameters  $f_{D^*D} = 140 \text{ keV}$  and  $M_{D^*D} = 3.91 \text{ GeV}$  given in Table III and the average values of  $f_D = 204(6) \text{ MeV}$  and  $f_{D^*} = 250(8) \text{ MeV}$  from [28,93]. We have neglected the equal and small contributions to the two sum rules from the QCD continuum above the continuum threshold taken to be  $t_c \approx 30 \text{ GeV}^2$ , which is the mean of the two extremal values delimiting the stability region. These results indicate that

1. For finite  $N_c$ , the nonresonant contribution is about one order of magnitude smaller than the one of the resonance molecule (a similar conclusion using an alternative approach has been reached in [87]) and disprove the claim of Ref. [60] based on large  $N_c$  once an appropriate matching of the two correlators via the  $k^2$  factor is done.
2. *A posteriori*, the existence of the stability region or “sum rule window” in the LSR analysis where one can extract the (postulated) resonance mass and coupling using the spectral function parametrization within the duality ansatz “one resonance” +QCD continuum is a strong indication of the duality between the QCD-OPE and the phenomenological side of the sum rule, where the resonance contribution is dominant over the one of the nonresonant states. This fact does not also support the claim of Ref. [60].

## XI. RADIAL EXCITATIONS

We present in this section a new estimate of the couplings and masses of the first radial excitations using the lowest moments  $\mathcal{L}_0^c$  and  $\mathcal{R}_0^c$ .<sup>9</sup> In so doing, we use a “two resonance” parametrization of the spectral function.

### A. The $(D^*D)_1$ first radial excitation

We insert the previously obtained values of the lowest ground state  $D^*D$  mass and coupling and study the  $\tau$  and  $t_c$

<sup>9</sup>We note that the moment  $\mathcal{R}_1^c$ , which is expected to be more sensitive to the radial excitation contribution, has a behavior similar to  $\mathcal{R}_0^c$  and will not be presented here.



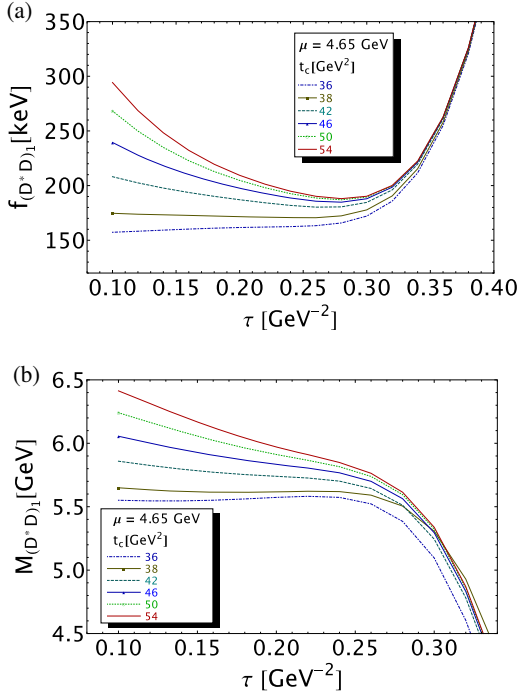


FIG. 21.  $f_{(D^*D)_1}$  and  $M_{(D^*D)_1}$  as function of  $\tau$  at NLO for different values of  $t_c$ , for  $\mu = 4.65$  GeV and for values of  $\bar{m}_c(\bar{m}_c)$  given in Table II.

stability of the sum rules by fixing the subtraction constant  $\mu$  as in Eq. (15). The analysis is shown in Fig. 21 where the stability region is delimited by  $t_c = 39$  and  $50$   $\text{GeV}^2$  to which corresponds respectively the  $\tau$  stability of (0.14–0.18) and (0.28–0.29)  $\text{GeV}^{-2}$ . The results,

$$f_{(D^*D)_1} = 197(25) \text{ keV}, \quad M_{(D^*D)_1} = 5709(70) \text{ MeV}, \quad (33)$$

TABLE V. Sources of errors and predictions from LSR at NLO and for the decay constants and masses of the molecules and tetraquark radial excitation states. The errors from the QCD input parameters are from Table II. We take  $|\Delta\tau| = 0.01$   $\text{GeV}^{-2}$  and  $\Delta\mu = 0.05$  GeV. The quoted errors have been estimated fixing  $t_c$  at the mean of the two extremal values delimiting the stability region quoted in Table VI. We notice that the relative large values of some individual errors in the case of  $D_s^*D_s$  and  $(D_0^*D_1)_1$  are mainly induced by the shift of the position of the minima compared to the one of the central values.

Observables	$\Delta t_c$	$\Delta\tau$	$\Delta\mu$	$\Delta\alpha_s$	$\Delta PT$	$\Delta m_s$	$\Delta m_c$	$\Delta\bar{\psi}\psi$	$\Delta\kappa$	$\Delta G^2$	$\Delta M_0^2$	$\Delta\bar{\psi}\psi^2$	$\Delta G^3$	$\Delta OPE$	$\Delta M_G$	$\Delta f_G$	$\Delta M_{(G)_1}$	Values
Coupling $f_G$ [keV]																		
$(D^*D)_0$	21	0.7	2.9	11	6.2	...	8.5	8.2	...	0.09	4.5	26.8	0.10	19	14.5	34	...	46(56)
$(D^*D)_1$	10.0	0.18	1.35	8.5	0.60	...	5.60	9.30	...	0.06	3.70	7.40	0.07	3.71	1.80	15.1	10.1	197(25)
$(D_0^*D_1)_1$	5.2	0.5	0.4	4.3	9.3	...	4.7	19.25	...	0.10	6.30	10.5	0.28	9.10	0.45	16.5	26.0	238(41)
$(A_{cd})_1$	18.9	0.12	2.29	11.8	9.60	...	7.31	9.49	...	0.04	6.04	7.43	0.15	6.41	4.05	15.1	17.2	272(38)
$(D_s^*D)_1$	9.0	0.20	1.50	8.8	0.20	0.95	4.90	8.65	10.5	0.06	2.20	6.9	0.08	6.1	1.75	16.8	8.70	199(29)
$(D_s^*D_s)_1$	6.5	0.60	1.80	9.5	4.9	1.5	4.6	11.7	13.0	0.18	4.80	10.0	0.20	12.4	7.30	16.2	27.1	197(43)
Mass $M_G$ [MeV]																		
$(D^*D)_1$	30.0	38.9	11.8	5.0	0.02	...	16.5	10.0	...	1.10	29.5	6.0	1.15	23.0	18.0	12	...	5709(70)
$(D_0^*D_1)_1$	83.0	2.5	0.4	10	14	...	11.8	55.2	...	0.2	34	74.6	0.7	50.6	20.8	55	...	6375(152)
$(A_{cd})_1$	59.0	15.2	9.46	6.54	3.81	...	19.1	26.4	...	0.15	22.5	4.96	0.80	14.3	20.7	26.5	...	5717(82)
$(D_s^*D)_1$	2.0	30.0	16.5	7.5	0.02	2.0	18.5	13.0	6.0	0.85	20.5	4.0	1.40	10.0	19.0	10	...	5725(52)
$(D_s^*D_s)_1$	42.0	49.0	39.5	42.5	1.05	4.5	20.5	38.5	45.5	1.0	35.0	58.0	3.0	40.8	25.5	69.0	...	5786(152)

are quoted in Table V. The set of  $(t_c, \tau)$  is compiled in Table VI.

One can notice that the mass value is roughly about the (expected) one of  $\sqrt{t_c} \simeq (4.7\text{--}6.2)$  GeV inside the stability region where the lowest ground state mass has been extracted.

### B. The $(D_0^*D_1)_1$ radial excitation

We show the analysis in Fig. 22. The curves have similar behavior as in the case of  $(D^*D)_1$ , but the stabilities are reached for higher values of  $t_c$  which imply a higher value of the  $(D_0^*D_1)_1$  radial excitation mass. The results are quoted in Table V and the set of  $(t_c, \tau)$  is compiled in Table VI.

### C. The $(A_{cd})_1$ radial excitation

The behaviors of the coupling and mass versus  $\tau$  and  $t_c$  are similar to the case of the one of  $(D^*D)_1$  and will not be repeated here. The results are quoted in Table V.

### D. The $(D_s^*D)_1$ radial excitation

We estimate the mass and coupling of the  $(D_s^*D)_1$  radial excitation like in the case of  $(D^*D)_1$ . The analysis is similar and the curves have the same behaviors. The set of LSR parameters used to get the results are quoted in Table VI. We obtain the results quoted in Tables V:

$$f_{(D_s^*D)_1} = 199(29) \text{ keV}, \quad M_{(D_s^*D)_1} = 5725(52) \text{ MeV}, \quad (34)$$

where they are also quite high compared to the ones of ordinary mesons.

TABLE VI. Values of the set of the LSR parameters  $(t_c, \tau)$  at the optimization region for the PT series up to NLO and for the OPE truncated at the dimension-6 condensates and for  $\mu = 4.65$  GeV. The first set for  $(D_0^* D_1)_1$  and  $(A_c)_1$  correspond, respectively, to the mass and coupling.

States	$(1^+)$ radial excitations					
Parameters	$(D^* D)_0$	$(D^* D)_1$	$(D_0^* D_1)_1$	$(A_c)_1$	$(D_s^* D)_1$	$(D_s^* D_s)_1$
$t_c$ [GeV <sup>2</sup> ]	27–46	39–50	48–56	39–50	40–50	42–52
$\tau$ [GeV <sup>-2</sup> ] $10^2$	30; 34	13; 26	15, 24; 20, 25	7, 26; 29, 27	9; 27	21; 29

### E. The first radial excitation $(D_s^* D_s)_1$

In this subsection, we study the first radial excitation  $(D_s^* D_s)_1$ . The  $\tau$  and  $t_c$  behaviors of its mass and coupling are shown in Fig. 23 for  $\mu = 4.65$  GeV. The  $\tau$  and  $t_c$  stabilities are reached for the set  $(\tau, t_c) = (0.28, 42)$  to  $(0.30, 54)$  in units of (GeV<sup>-2</sup>, GeV<sup>2</sup>). We deduce (see Table V):

$$f_{(D_s^* D_s)_1} = 197(43) \text{ keV}, \quad M_{(D_s^* D_s)_1} = 5786(152) \text{ MeV}. \quad (35)$$

One can notice that the coupling of the first radial excitation is similar to the previous radial excited states that are relatively large compared to the ones of lowest ground states. This feature differs from the case of ordinary mesons built from bilinear currents. The mass is also found to be relatively high.

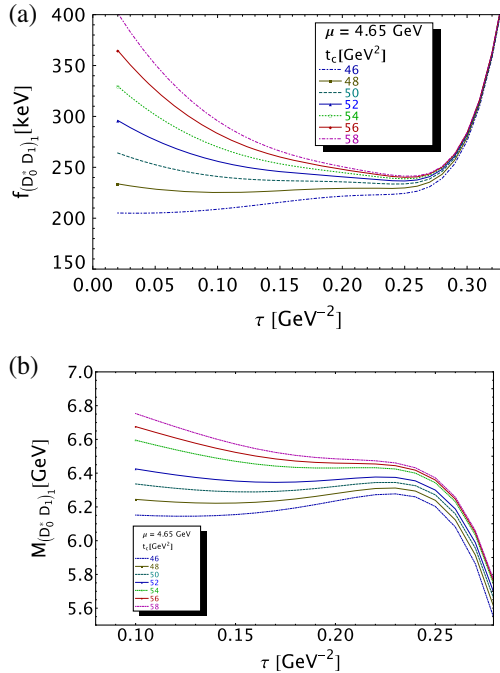


FIG. 22.  $f_{(D_0^* D_1)_1}$  and  $M_{(D_0^* D_1)_1}$  as function of  $\tau$  at NLO for different values of  $t_c$  and for  $\mu = 4.65$  GeV.

### F. Comments on the radial excitations

We have shown previously that the couplings of the excited states to the corresponding currents are as large as the one of the ground states (see Table V), which is a new feature compared to the case of ordinary hadrons.

We have also shown that the mass-splittings between the first radial excitation and the lowest ground state are (see Table V)

$$M_{(G)_1} - M_G \simeq (1.70 \sim 2.35) \text{ GeV}, \quad (36)$$

which is much bigger than the one (500 ~ 600) MeV for ordinary mesons but comparable with the one obtained for the  $DK$  state in [44]. The authors in Ref. [88] have also noticed a such anomalously large value of the mass of the radial excitation  $M_{R1} \approx \sqrt{t_c} \geq 4.5$  GeV in the analysis of the  $Z_c(4020, 4025)$ . Then, they have concluded that the  $Z_c(4020, 4025)$  cannot be a tetraquark state as the value of  $t_c$  used to extract these masses is much larger than the one expected from the empirical relation

$$\sqrt{t_c} \approx M_{Z_c} + 0.5 \text{ GeV}, \quad (37)$$

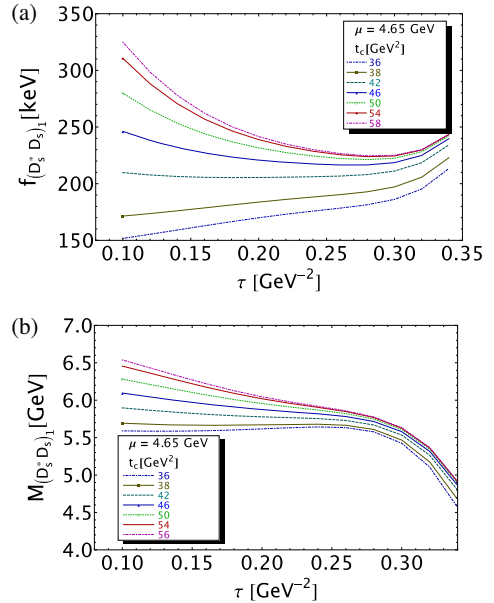


FIG. 23.  $f_{(D_s^* D_s)_1}$  and  $M_{(D_s^* D_s)_1}$  as function of  $\tau$  at NLO for different values of  $t_c$  and for  $\mu = 4.65$  GeV.

where the value 0.5 GeV has been inspired from ordinary mesons and from the results of [94].

From our result, one can already conclude that the  $Z_c(4020)$  to  $Z_c(4430)$  are too low to be the radial excitations of the  $Z_c(3900)$  unless they couple weakly to the interpolating current such that their effect is tiny in the LSR analysis.

### G. Can there be a weakly coupled radial excitation?

If one literally extrapolates the phenomenological observation from ordinary hadrons, one would expect a radial excitation with a mass

$$M_{(D^*D)_0} \approx M_{D^*D} + 0.5 \text{ GeV} \simeq 4.4 \text{ GeV}, \quad (38)$$

which is relatively low compared to the previous prediction in Eq. (33) but seems to fit the  $Z_c(4430)$ . To understand why it can have been eventually missed in the previous analysis, we shall determine the  $Z_c(4430)$  coupling to the current and use as input the experimental mass value.<sup>10</sup>

In so doing, we reconsider the  $\mathcal{L}_0^c$  moment. We use a two-resonance parametrization of the spectral function and introduce as inputs the previous values of the  $D^*D$  molecule mass and coupling. We use the experimental mass of the  $Z_c(4430)$ . We include the *high-mass*  $(D^*D)_1$  radial excitation obtained previously into the QCD continuum contribution.

We show the  $\tau$  behavior of the coupling for different  $t_c$  values and for fixed  $\mu = 4.65$  GeV in Fig. 24. At the  $(\tau, t_c)$  stability regions (0.30,27) to (0.34,46) ( $\text{GeV}^{-2}$ ,  $\text{GeV}^2$ ), we deduce

$$f_{(D^*D)_0} = 46(56) \text{ keV}, \quad (39)$$

where the different sources of the errors are given in Table V. The coupling is indeed relatively small compared to that of  $f_{D^*D} = 140$  keV. It can even be consistent with zero due to the large errors mainly induced by the coupling of the ground state and of the dimension-6 condensates. This result may support an eventual radial excitation interpretation of the  $Z(4340)$  which couples very weakly to the current and having a mass much lower than the strongly coupled [ $f_{(D^*D)_1} = 197$  MeV] radial excitation with a mass 5709 MeV (see Table V). This weak coupling disagrees with the one obtained in Ref. [95] and may originate from the fact that the latter analysis has been done at a smaller value of  $t_c$  and at the scale  $\mu = 1.5$  GeV which is too low compared to the optimal choice obtained in the present work. However, as we have already mentioned in Sec. VI B, we do not find any convincing theoretical basis for justifying this low choice of  $\mu$ . We expect that similar results can be obtained in some other channels.

<sup>10</sup>No stability region is obtained for an the attempt to determine this mass from the LSR  $\mathcal{R}_0^c$ .

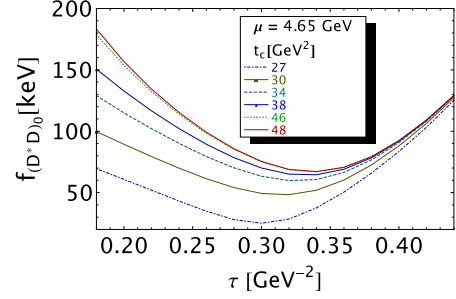


FIG. 24. The coupling  $f_{(D^*D)_0}$  of the  $Z_c(4430)$  at NLO as a function of  $\tau$  for different values of  $t_c$  and for  $\mu = 4.65$  GeV.

## XII. VERSUS OUR PREVIOUS RESULTS

We compare our results with our previous ones from Refs. [23,24] in Table VII. Notice that, in [23], the double ratio of moments has been also used to extract directly the  $SU(3)$  breaking contributions to the masses and couplings. One can notice a good agreement between the different results. The exception is the central value of  $M_{D_0^*D_1}$ , which slightly moves in the three papers though the results are in agreement within the errors. This is due to the difficult localization of the inflexion point which we have identified in the present work with the minimum of the coupling like in some other channels.

## XIII. CONFRONTATION WITH THE DATA

As proposed in [44], we consider that the physical states are superposition of quasidegenerated hypothetical molecules and tetraquark states having the same quantum numbers  $J^{PC}$  and having almost the same coupling strength to the currents. We have denoted these observed states as tetramoles  $\mathcal{T}$  (tetraquarks  $\oplus$  molecules).

### A. $Z_c(3900)$ as a tetramole state

One may define the tetramole  $\mathcal{T}_c$  as a superposition of the  $D^*D$  molecule and  $A_{cd}$  tetraquark state with the parameters:

$$M_{\mathcal{T}_c} = 3900(42) \text{ MeV}, \quad f_{\mathcal{T}_c} = 155(11) \text{ keV}, \quad (40)$$

which are the mean of the two previous couplings and masses. We identify this tetramole state with the  $Z_c(3900)$  found by BELLE [79] and BESIII [80].

### B. $Z_c(4025,4050)$ as a $D_0^*D_1$ molecule

The  $D_0^*D_1$  molecule with the parameters

$$M_{D_0^*D_1} = 4023(130) \text{ MeV}, \quad f_{D_0^*D_1} = 96(23) \text{ keV}, \quad (41)$$

as given in Tables VII and III, might be identified with the  $Z_c(4025)$  found by BES [82] or with the  $Z_c(4050)$  found

TABLE VII. Summary of the couplings and masses predictions of the lowest ground states and comparison with our previous results in Refs. [23,24].

States	Couplings			Masses		
	Ref. [24]	Ref. [23]	New	Ref. [24]	Ref. [23]	New
Molecule $(\bar{c}d)(c\bar{u})$						
$D^*D$	154(7)	...	140(15)	3901(62)	...	3912(61)
$D_0^*D_1$	96(15)	...	96(23)	4394(164)	3854(182)	4023(130)
Tetraquark $(\bar{c}\bar{d})(cu)$						
$A_{cd}$	176(30)	...	173(17)	3890(130)	...	3889(42)
Molecule $(c\bar{s})(\bar{c}u)$						
$D_s^*D$	...	...	130(15)	...	...	3986(51)
$D^*D_s$	...	...	133(16)	...	...	3979(56)
$D_{s0}^*D_1$	...	...	86(23)	...	...	4064(133)
$D_0^*D_{s1}$	...	...	89(22)	...	...	4070(133)
Tetraquark $(\bar{c}\bar{s})(cu)$						
$A_{cs}$	...	...	148(17)	...	...	3950(56)
Molecule $(\bar{c}s)(c\bar{s})$						
$D_s^*D_s$	...	114(13)	...	...	3901(62)	4091(57)
$D_{s0}^*D_{s1}$	...	79(14)	70(16)	...	4269(205)	4198(129)
$A_{css}$	...	114(16)	131(14)	...	4209(112)	4014(86)

by BELLE [83]. However, one should mention that these states are not well established and have not yet been retained in the PDG summary table [65].

### C. $Z_c(4430)$ as a weakly coupled radial excitation?

Pursuing our confrontation with the data, we note that the  $Z_c(4430)$  [85,86] is too low to be the strongly coupled [ $f_{(D^*D)_1} = 196(41)$  MeV] first radial excitation of the  $D^*D$  expected to be in the range (5.4 ~ 5.8) GeV (see Table III). However, it can be fitted by the weakly coupled [ $f_{(D^*D)_0} = 46(56)$  MeV] low mass one obtained in Sec. XI G.

### D. The $Z_{cs}(3983)$ as a tetramole

We consider the tetramole  $\mathcal{T}_s$  as the combination of the  $D_s^*D$ ,  $D^*D_s$  molecules and  $A_{cs}$  tetraquark states have almost the same mass and same coupling to the currents (see Table III). Taking the mean values of these parameters, we obtain

$$M_{\mathcal{T}_{cs}} = 3973(31) \text{ MeV}, \quad f_{\mathcal{T}_{cs}} = 136(9) \text{ keV}, \quad (42)$$

which we can identify with the recent  $Z_{cs}(3983)$  found recently by BESIII [45].

### E. The $Z_{cs}(4100)$ bump as a $D_{s0}^*D_1 \oplus D_0^*D_{s1}$ molecule

Inspecting our predictions for the  $D_{s0}^*D_1$  and  $D_0^*D_{s1}$  masses in Tables III and VII, we find that they are almost degenerated and have almost the same couplings. Taking their combination having a mean mass,

$$\begin{aligned} M_{D_{s0}^*D_1 \oplus D_0^*D_{s1}} &= 4067(94) \text{ MeV}, \\ f_{D_{s0}^*D_1 \oplus D_0^*D_{s1}} &= 88(16) \text{ keV}, \end{aligned} \quad (43)$$

we are tempted to identify this state with the  $Z_{cs}(4100)$  bump observed by BESIII [45]. Its relatively small coupling to the current compared to the one of the ground state  $Z_{cs}(3983)$  may indicate that it can be large using a Golberger-Treiman-type relation argument where the hadronic coupling behaves as the inverse of coupling (see, e.g., [96]).

### F. The future $Z_{css}$ states

From our predictions in Table III, one can also define a tetramole  $\mathcal{T}_{css}$ , which is a superposition of the  $D_s^*D_s$  molecule and  $A_{css}$  tetraquark states, with

$$M_{\mathcal{T}_{css}} = 4068(48) \text{ MeV}, \quad f_{\mathcal{T}_{css}} = 114(10) \text{ keV}. \quad (44)$$

One also expects to have a  $D_{s0}^*D_{s1}$  molecule at a higher mass value:

$$M_{D_{s0}^*D_{s1}} = 4198(129) \text{ MeV}, \quad f_{D_{s0}^*D_{s1}} = 79(14) \text{ keV}, \quad (45)$$

where its coupling to the current is relatively small, indicating that it can be relatively large using a Golberger-Treiman-type relation argument where the hadronic coupling behaves as  $1/f_{D_{s0}^*D_{s1}}$  (see, e.g., [96]).



These predicted states are expected to be seen in the near future experiments and can be considered as a test of the predictions given in this paper.

#### XIV. ON SOME OTHER AND LSR RESULTS

After the publication of the recent BESIII results on the observation of the  $Z_{cs}(3982)$  candidate [45], many papers using different models appear in the literature [97] for attempts to explain the true nature of this state.

Besides the pioneer QSSR estimate of the  $D^*D_s$  molecule and tetraquark states [98],<sup>11</sup> some recent papers using LSR come to our attention (see, e.g., [99]) where we notice some common caveats:

1. All analysis is done at LO of perturbation theory where the choice of the value of the  $\overline{MS}$  running mass in favor of the pole mass is unjustified because the definitions of the two masses are undistinguishable at this order. Moreover, the calculation of the spectral functions using on shell renormalization would (*a priori*) favor the choice of the on shell mass. The difference on the effect of this choice is explicitly shown in Fig. 13. Hopefully, the effects of NLO corrections in the  $\overline{MS}$  scheme are tiny (see Fig. 13) in the LSR analysis confirming (*a posteriori*) the intuitive choice of the  $\overline{MS}$  running mass at LO.
2. The value of  $t_c \equiv s_0$  used to determine the mass and coupling of about  $(18 \sim 23) \text{ GeV}^2$  is relatively low as it corresponds to the beginning of the  $\tau$ -stability region (see previous figures), where one also notices that the predictions increase until the  $t_c$ -stability value. As a consequence, the absolute value and the error in the extraction of the mass and coupling have been underestimated.
3. In general, the way how the errors from different sources have been estimated are not explained in details, which raises some doubts on the real size of the quoted errors having in mind that the extraction of the different errors quoted in Tables III and V require some painful works.
4. The value of the four-quark condensates from the vacuum saturation assumption is often used. However, though this estimate is correct in the large  $N_c$  limit, it has been found phenomenologically from different light quarks and  $\tau$ -decay channels [36,48–52] that this estimate is largely violated at the realistic case  $N_c = 3$ . Moreover, it is also known that the dimension-6 quark condensates which mix under renormalization [46] (Part VII, page 285) does not support the previous assumption.
5. The previous papers extend the OPE to high dimensions up to  $d = 10$  vacuum condensates but

only for some classes of high-dimension condensate contributions and by assuming the validity of the factorization assumption for estimating their sizes. However, it has been shown in [27,46] (Part VII, page 285) that the structure of these high-dimension condensates are quite complex due to their mixing under renormalization such that their inclusion in the QSSR analysis should deserve more care.

In addition to these caveats, we also notice that

1. Differentiating the neutral from the charged  $Z_{cs}$  is purely academic from the approach as the two states are almost degenerated within the errors.
2. In Refs. [87,88], the author introduces a relation between the PT subtraction scale  $\mu$  and the so-called energy bound which is quite obscure to us as discussed in Sec. VI B.

#### XV. SUMMARY AND CONCLUSIONS

We have done the following in this paper:

1. Systematically studied the spectra and couplings of the  $(\bar{c}q)(\bar{q}'c)$  molecules and  $(\bar{c}\bar{q})(q'c)$  tetraquark states where  $q, q' \equiv d, s$  are light quarks.
2. Improved our previous predictions obtained in Refs. [23,24] by a much better localization of the  $t_c$ -,  $\tau$ -, and  $\mu$ -stability points and by using updated values of some QCD input parameters.
3. Emphasized that the localization of the inflexion point for extracting the values of the masses can be fixed more precisely in most channels by identifying it with the value of  $\tau$  corresponding to the minimum of the curve where optimal value of the coupling is extracted.
4. Provided new predictions of the  $(\bar{c}q)(\bar{s}c)$  molecules and  $(\bar{c}\bar{q})(sc)$  tetraquark states.
5. Introduced the tetramole states as a superposition of quasidegenerated molecules and tetraquark states having the same quantum numbers  $J^{PC}$  with almost the same couplings strengths to the interpolating currents. It is remarkable to notice that the mass splittings of the tetramoles  $\mathcal{T}_c$ ,  $\mathcal{T}_{cs}$ , and  $\mathcal{T}_{css}$  due to  $SU(3)$  breakings are successively about  $(73 \sim 91) \text{ MeV}$ .
6. Completed the analysis with new predictions of some first radial excitation masses and couplings. One can notice that the mass gap of about  $(1.7 \sim 2.35) \text{ GeV}$ , between the lowest mass ground state and the first radial excitation strongly coupled to the current, is quite large compared to  $(0.5 \sim 0.7) \text{ GeV}$  for ordinary  $\bar{q}q$  mesons. Similar results have been obtained for the  $DK$ -like states [44]. However, a weakly coupled radial excitation (see Sec. XI G) having a lower mass of about  $4.4 \text{ GeV}$  is not excluded from the approach. These features may signal some new dynamics of these exotic states which can be found in these high-mass regions.

<sup>11</sup>For more complete references, see, e.g., [14].

7. Compared successfully our predictions with the observed  $Z_c$  and  $Z_{cs}$  spectra.
8. Given new predictions for the future  $Z_{css}$  states.
9. Also shown that a result based on a qualitative  $N_c$  counting without taking into account the dynamics from Feynman loop calculation leads to a wrong conclusion.

### ACKNOWLEDGMENTS

We thank Professor G. Veneziano for discussions and comments on the manuscript.

### APPENDIX: QCD SPECTRAL FUNCTIONS WITH $J^P = 1^+$

We shall present in the following the different QCD expressions of the spectral functions related to the molecular and tetraquarks currents, which come from the evaluation of the two-point correlation function using the  $J^P = 1^+$  hadronic currents given in Table I where  $q \equiv s$ . The expressions obtained in the chiral limit  $m_s = m_d = 0$  can be found in Ref. [24] while the one with a double strange quarks has been obtained in [23]. We have used the expression of the  $\langle G^3 \rangle$  condensate contribution obtained in

the chiral limit in [24], which will not be given below. One should notice that, compared to the QCD expressions given in the literature, the ones that we give below and in the two previous papers [23,24] are completely integrated and compact. Hereafter, we define  $\rho(t) \equiv \frac{1}{\pi} \text{Im}\Pi^{(1)}(t)$ , where  $\text{Im}\Pi(t)^{(1)}$  is the spectral function defined in Eq. (5), with

$$\rho(t) \simeq \rho^{\text{pert}} + \rho^{\langle \bar{q}q \rangle} + \rho^{\langle G^2 \rangle} + \rho^{\langle \bar{q}Gq \rangle} + \rho^{\langle \bar{q}q \rangle^2} + \rho^{\langle G^3 \rangle}, \quad (\text{A1})$$

where  $\langle G^2 \rangle \equiv \langle g^2 G^2 \rangle$ ,  $\langle \bar{q}Gq \rangle \equiv M_0^2 \langle \bar{q}q \rangle$ ,  $\langle G^3 \rangle \equiv \langle g^3 G^3 \rangle$ , and  $x \equiv m_c^2/t$ ,  $v = \sqrt{1-4x}$ ,  $\mathcal{L}_v = \ln \frac{(1+v)}{(1-v)}$ ,  $\mathcal{L}_+ = \text{Li}_2(\frac{1+v}{2}) - \text{Li}_2(\frac{1-v}{2})$ .  $m_c \equiv M_c$  (respectively,  $m_s$ ) is the on shell charm (respectively, running strange) quark mass.  $b$  is the current mixing parameter where its optimal value is found to be  $b = 0$  [24]. For the estimate of the four-quark operator, we introduce the violation of the vacuum saturation estimate quantified by the factor  $\rho \simeq (3 \sim 4)$  defined in Table II.

### 1. The molecular currents

$D_s D^*$  molecule

$$\begin{aligned} \rho^{\text{pert}}(t) &= \frac{m_c^8}{5 \times 3 \times 2^{15} \pi^6} \left[ v \left( 840x + 140 + \frac{5248}{x} - \frac{1164}{x^2} - \frac{182}{x^3} + \frac{5}{x^4} \right) + 120 \mathcal{L}_v \left( 14x^2 + 15 - 18 \log(x) \right. \right. \\ &\quad \left. \left. - \frac{32}{x} + \frac{9}{x^2} \right) - 4320 \mathcal{L}_+ \right] - \frac{m_s m_c^7}{5 \times 2^{14} \pi^6} \left[ v \left( 420x + 70 + \frac{1574}{x} - \frac{257}{x^2} - \frac{16}{x^3} \right) \right. \\ &\quad \left. + 60 \mathcal{L}_v \left( 14x^2 + 4 - 12 \log(x) - \frac{16}{x} + \frac{3}{x^2} \right) - 1440 \mathcal{L}_+ \right], \\ \rho^{\langle \bar{q}q \rangle}(t) &= \frac{m_c^5 \langle \bar{s}s \rangle}{3 \times 2^{10} \pi^4} \left[ v \left( 60x + 10 - \frac{34}{x} - \frac{9}{x^2} \right) + 24 \mathcal{L}_v \left( 5x^2 - 3 + \frac{2}{x} \right) \right] + \frac{m_c^5 \langle \bar{q}q \rangle}{2^8 \pi^4} \left[ v \left( 6 - \frac{5}{x} - \frac{1}{x^2} \right) \right. \\ &\quad \left. + 6 \mathcal{L}_v \left( 2x - 2 + \frac{1}{x} \right) \right] + \frac{m_s m_c^4 \langle \bar{s}s \rangle}{2^{11} \pi^4} \left[ v \left( 12x + 2 - \frac{26}{x} + \frac{3}{x^2} \right) + 24 \mathcal{L}_v (x^2 + 1) \right] \\ &\quad - \frac{3m_s m_c^4 \langle \bar{q}q \rangle}{2^7 \pi^4} \left[ v \left( 2 + \frac{1}{x} \right) + 4 \mathcal{L}_v (x - 1) \right], \\ \rho^{\langle G^2 \rangle}(t) &= -\frac{m_c^4 \langle G^2 \rangle}{3^2 \times 2^{14} \pi^6} \left[ v \left( 60x - 62 + \frac{26}{x} + \frac{3}{x^2} \right) + 24 \mathcal{L}_v \left( 5x^2 - 6x + 3 - \frac{1}{x} \right) \right], \\ \rho^{\langle \bar{q}Gq \rangle}(t) &= -\frac{m_c^3 \langle \bar{s}Gs \rangle}{3 \times 2^{10} \pi^4} \left[ v \left( 66x + 11 - \frac{68}{x} \right) + 6 \mathcal{L}_v \left( 22x^2 + 3 + \frac{4}{x} \right) \right] + \frac{3m_c^3 \langle \bar{q}Gq \rangle}{2^9 \pi^4} \left( \frac{v}{x} - 2 \mathcal{L}_v \right) \\ &\quad - \frac{m_s m_c^2 \langle \bar{s}Gs \rangle}{3 \times 2^{10} \pi^4} \left[ v \left( 18x - 1 - \frac{8}{x} \right) + 18 \mathcal{L}_v (2x^2 + 1) \right] + \frac{3m_s m_c^2 \langle \bar{q}Gq \rangle}{2^8 \pi^4} v, \\ \rho^{\langle \bar{q}q \rangle^2}(t) &= \frac{m_c^2 \langle \bar{q}q \rangle \langle \bar{s}s \rangle}{64 \pi^2} v \left( 4 - \frac{m_s m_c \tau}{x} - \frac{m_s}{m_c} \right). \end{aligned} \quad (\text{A2})$$

$D_s^* D$  molecule

$$\begin{aligned}
\rho^{\text{pert}}(t) &= \frac{m_c^8}{5 \times 3 \times 2^{15} \pi^6} \left[ v \left( 840x + 140 + \frac{5248}{x} - \frac{1164}{x^2} - \frac{182}{x^3} + \frac{5}{x^4} \right) + 120\mathcal{L}_v \left( 14x^2 + 15 - 18 \log(x) \right. \right. \\
&\quad \left. \left. - \frac{32}{x} + \frac{9}{x^2} \right) - 4320\mathcal{L}_+ \right] - \frac{m_s m_c^7}{2^{12} \pi^6} \left[ v \left( 60 + \frac{130}{x} - \frac{18}{x^2} - \frac{1}{x^3} \right) \right. \\
&\quad \left. + 12\mathcal{L}_v \left( 10x - 4 - 6 \log(x) - \frac{6}{x} + \frac{1}{x^2} \right) - 144\mathcal{L}_+ \right], \\
\rho^{\langle \bar{q}q \rangle}(t) &= \frac{m_c^5 \langle \bar{s}s \rangle}{2^8 \pi^4} \left[ v \left( 6 - \frac{5}{x} - \frac{1}{x^2} \right) + 6\mathcal{L}_v \left( 2x - 2 + \frac{1}{x} \right) \right] + \frac{m_c^5 \langle \bar{q}q \rangle}{3 \times 2^{10} \pi^4} \left[ v \left( 60x + 10 - \frac{34}{x} - \frac{9}{x^2} \right) \right. \\
&\quad \left. + 24\mathcal{L}_v \left( 5x^2 - 3 + \frac{2}{x} \right) \right] + \frac{m_s m_c^4 \langle \bar{s}s \rangle}{2^{11} \pi^4} \left[ v \left( 12x + 2 - \frac{26}{x} + \frac{3}{x^2} \right) + 24\mathcal{L}_v(x^2 + 1) \right] \\
&\quad - \frac{3m_s m_c^4 \langle \bar{q}q \rangle}{2^7 \pi^4} \left[ v \left( 2 + \frac{1}{x} \right) + 4\mathcal{L}_v(x - 1) \right], \\
\rho^{\langle G^2 \rangle}(t) &= -\frac{m_c^4 \langle G^2 \rangle}{3^2 \times 2^{14} \pi^6} \left[ v \left( 60x - 62 + \frac{26}{x} + \frac{3}{x^2} \right) + 24\mathcal{L}_v \left( 5x^2 - 6x + 3 - \frac{1}{x} \right) \right], \\
\rho^{\langle \bar{q}Gq \rangle}(t) &= \frac{3m_c^3 \langle \bar{s}Gs \rangle}{2^9 \pi^4} \left( \frac{v}{x} - 2\mathcal{L}_v \right) - \frac{m_c^3 \langle \bar{q}Gq \rangle}{3 \cdot 2^{10} \pi^4} \left[ v \left( 66x + 11 - \frac{68}{x} \right) + 6\mathcal{L}_v \left( 22x^2 + 3 + \frac{4}{x} \right) \right] \\
&\quad - \frac{m_s m_c^2 \langle \bar{s}Gs \rangle}{2^{10} \pi^4} \left[ v \left( 2x - 25 + \frac{4}{x} \right) + 2\mathcal{L}_v(2x^2 - 24x + 9) \right] + \frac{3m_s m_c^2 \langle \bar{q}Gq \rangle}{2^8 \pi^4} v, \\
\rho^{\langle \bar{q}q \rangle^2}(t) &= \frac{m_c^2 \langle \bar{q}q \rangle \langle \bar{s}s \rangle}{64\pi^2} v \left( 4 - \frac{m_s m_c \tau}{x} \right). \tag{A3}
\end{aligned}$$

 $D_{s0}^* D_1$  molecule

$$\begin{aligned}
\rho^{\text{pert}}(t) &= \frac{m_c^8}{5 \times 3 \times 2^{15} \pi^6} \left[ v \left( 840x + 140 + \frac{5248}{x} - \frac{1164}{x^2} - \frac{182}{x^3} + \frac{5}{x^4} \right) + 120\mathcal{L}_v \left( 14x^2 + 15 - 18 \log(x) \right. \right. \\
&\quad \left. \left. - \frac{32}{x} + \frac{9}{x^2} \right) - 4320\mathcal{L}_+ \right] + \frac{m_s m_c^7}{5 \times 2^{14} \pi^6} \left[ v \left( 420x + 70 + \frac{1574}{x} - \frac{257}{x^2} - \frac{16}{x^3} \right) \right. \\
&\quad \left. + 60\mathcal{L}_v \left( 14x^2 + 4 - 12 \log(x) - \frac{16}{x} + \frac{3}{x^2} \right) - 1440\mathcal{L}_+ \right], \tag{A4} \\
\rho^{\langle \bar{q}q \rangle}(t) &= -\frac{m_c^5 \langle \bar{q}q \rangle}{2^8 \pi^4} \left[ v \left( 6 - \frac{5}{x} - \frac{1}{x^2} \right) + 6\mathcal{L}_v \left( 2x - 2 + \frac{1}{x} \right) \right] - \frac{m_c^5 \langle \bar{s}s \rangle}{3 \times 2^{10} \pi^4} \left[ v \left( 60x + 10 - \frac{34}{x} - \frac{9}{x^2} \right) \right. \\
&\quad \left. + 24\mathcal{L}_v \left( 5x^2 - 3 + \frac{2}{x} \right) \right] - \frac{3m_s m_c^4 \langle \bar{q}q \rangle}{2^7 \pi^4} \left[ v \left( 2 + \frac{1}{x} \right) + 4\mathcal{L}_v(x - 1) \right] \\
&\quad + \frac{m_s m_c^4 \langle \bar{s}s \rangle}{2^{11} \pi^4} \left[ v \left( 12x + 2 - \frac{26}{x} + \frac{3}{x^2} \right) + 24\mathcal{L}_v(x^2 + 1) \right], \\
\rho^{\langle G^2 \rangle}(t) &= -\frac{m_c^4 \langle G^2 \rangle}{3^2 \times 2^{14} \pi^6} \left[ v \left( 60x - 62 + \frac{26}{x} + \frac{3}{x^2} \right) + 24\mathcal{L}_v \left( 5x^2 - 6x + 3 - \frac{1}{x} \right) \right], \\
\rho^{\langle \bar{q}Gq \rangle}(t) &= -\frac{3m_c^3 \langle \bar{q}Gq \rangle}{2^9 \pi^4} \left( \frac{v}{x} - 2\mathcal{L}_v \right) + \frac{m_c^3 \langle \bar{s}Gs \rangle}{3 \times 2^{10} \pi^4} \left[ v \left( 66x + 11 - \frac{68}{x} \right) + 6\mathcal{L}_v \left( 22x^2 + 3 + \frac{4}{x} \right) \right] \\
&\quad + \frac{3m_s m_c^2 \langle \bar{q}Gq \rangle}{2^8 \pi^4} v - \frac{m_s m_c^2 \langle \bar{s}Gs \rangle}{3 \times 2^{10} \pi^4} \left[ v \left( 18x - 1 - \frac{8}{x} \right) + 18\mathcal{L}_v(2x^2 + 1) \right], \\
\rho^{\langle \bar{q}q \rangle^2}(t) &= \frac{\langle \bar{q}q \rangle \langle \bar{s}s \rangle}{64\pi^2} v \left[ 4m_c^2 + m_s m_c \left( 1 + \frac{m_c^2 \tau}{x} \right) \right]. \tag{A5}
\end{aligned}$$

$D_0^* D_{s1}$  molecule

$$\begin{aligned}
\rho^{\text{pert}}(t) &= \frac{m_c^8}{5 \times 3 \times 2^{15} \pi^6} \left[ v \left( 840x + 140 + \frac{5248}{x} - \frac{1164}{x^2} - \frac{182}{x^3} + \frac{5}{x^4} \right) + 120 \mathcal{L}_v \left( 14x^2 + 15 - 18 \log(x) - \frac{32}{x} + \frac{9}{x^2} \right) \right. \\
&\quad \left. - 4320 \mathcal{L}_+ \right] + \frac{m_s m_c^7}{2^{12} \pi^6} \left[ v \left( 60 + \frac{130}{x} - \frac{18}{x^2} - \frac{1}{x^3} \right) + 12 \mathcal{L}_v \left( 10x - 4 - 6 \log(x) - \frac{6}{x} + \frac{1}{x^2} \right) - 144 \mathcal{L}_+ \right], \\
\rho^{\langle \bar{q}q \rangle}(t) &= -\frac{m_c^5 \langle \bar{q}q \rangle}{3 \times 2^{10} \pi^4} \left[ v \left( 60x + 10 - \frac{34}{x} - \frac{9}{x^2} \right) + 24 \mathcal{L}_v \left( 5x^2 - 3 + \frac{2}{x} \right) \right] \\
&\quad - \frac{m_c^5 \langle \bar{s}s \rangle}{2^8 \pi^4} \left[ v \left( 6 - \frac{5}{x} - \frac{1}{x^2} \right) + 6 \mathcal{L}_v \left( 2x - 2 + \frac{1}{x} \right) \right] - \frac{3m_s m_c^4 \langle \bar{q}q \rangle}{2^7 \pi^4} \left[ v \left( 2 + \frac{1}{x} \right) + 4 \mathcal{L}_v(x-1) \right] \\
&\quad + \frac{m_s m_c^4 \langle \bar{s}s \rangle}{2^{11} \pi^4} \left[ v \left( 12x + 2 - \frac{26}{x} + \frac{3}{x^2} \right) + 24 \mathcal{L}_v(x^2 + 1) \right], \\
\rho^{\langle G^2 \rangle}(t) &= -\frac{m_c^4 \langle G^2 \rangle}{3^2 \times 2^{14} \pi^6} \left[ v \left( 60x - 62 + \frac{26}{x} + \frac{3}{x^2} \right) + 24 \mathcal{L}_v \left( 5x^2 - 6x + 3 - \frac{1}{x} \right) \right], \\
\rho^{\langle \bar{q}Gq \rangle}(t) &= \frac{m_c^3 \langle \bar{q}Gq \rangle}{2^{10} \pi^4} \left[ v \left( 30x + 5 + \frac{4}{x} \right) + 6 \mathcal{L}_v(10x^2 - 3) \right] - \frac{3m_c^3 \langle \bar{s}Gs \rangle}{2^9 \pi^4} \left( \frac{v}{x} - 2 \mathcal{L}_v \right) \\
&\quad + \frac{3m_s m_c^2 \langle \bar{q}Gq \rangle}{2^8 \pi^4} [3v + 2 \mathcal{L}_v(2x - 1)] - \frac{m_s m_c^2 \langle \bar{s}Gs \rangle}{2^{10} \pi^4} \left[ v \left( 2x - 1 + \frac{4}{x} \right) + 2 \mathcal{L}_v(2x^2 - 3) \right], \\
\rho^{\langle \bar{q}q \rangle^2}(t) &= \frac{m_c^2 \langle \bar{q}q \rangle \langle \bar{s}s \rangle}{64 \pi^2} v \left[ 4 + \frac{m_s m_c \tau}{x} \right]. \tag{A6}
\end{aligned}$$

## 2. The tetraquark current $A_{cd}$

$$\begin{aligned}
\rho^{\text{pert}}(t) &= \frac{m_c^8(1+b^2)}{5 \times 3^2 \times 2^{13} \pi^6} \left[ v \left( 840x + 140 + \frac{5248}{x} - \frac{1164}{x^2} - \frac{182}{x^3} + \frac{5}{x^4} \right) + 120 \mathcal{L}_v \left( 14x^2 + 15 - 18 \log(x) \right. \right. \\
&\quad \left. \left. - \frac{32}{x} + \frac{9}{x^2} \right) - 4320 \mathcal{L}_+ \right] - \frac{m_s m_c^7(1-b^2)}{5 \times 3 \times 2^{12} \pi^6} \left[ v \left( 420x + 70 + \frac{1574}{x} - \frac{257}{x^2} - \frac{16}{x^3} \right) \right. \\
&\quad \left. + 60 \mathcal{L}_v \left( 14x^2 + 4 - 12 \log(x) - \frac{16}{x} + \frac{3}{x^2} \right) - 1440 \mathcal{L}_+ \right], \tag{A7} \\
\rho^{\langle \bar{q}q \rangle}(t) &= \frac{m_c^5(1-b^2) \langle \bar{q}q \rangle}{3 \times 2^6 \pi^4} \left[ v \left( 6 - \frac{5}{x} - \frac{1}{x^2} \right) + 6 \mathcal{L}_v \left( 2x - 2 + \frac{1}{x} \right) \right] + \frac{m_c^5(1-b^2) \langle \bar{s}s \rangle}{3^2 \times 2^8 \pi^4} \left[ v \left( 60x + 10 - \frac{34}{x} - \frac{9}{x^2} \right) \right. \\
&\quad \left. + 24 \mathcal{L}_v \left( 5x^2 - 3 + \frac{2}{x} \right) \right] - \frac{m_s m_c^4(1+b^2) \langle \bar{q}q \rangle}{2^5 \pi^4} \left[ v \left( 2 + \frac{1}{x} \right) - 4 \mathcal{L}_v(1-x) \right] \\
&\quad + \frac{m_s m_c^4(1+b^2) \langle \bar{s}s \rangle}{3 \times 2^9 \pi^4} \left[ v \left( 12x + 2 - \frac{26}{x} + \frac{3}{x^2} \right) + 24 \mathcal{L}_v(x^2 + 1) \right], \\
\rho^{\langle G^2 \rangle}(t) &= \frac{m_c^4(1+b^2) \langle G^2 \rangle}{3^2 \times 2^{11} \pi^6} \left[ v \left( 6 - \frac{5}{x} - \frac{1}{x^2} \right) + 6 \mathcal{L}_v \left( 2x - 2 + \frac{1}{x} \right) \right], \\
\rho^{\langle \bar{q}Gq \rangle}(t) &= \frac{m_c^3(1-b^2) \langle \bar{q}Gq \rangle}{2^7 \pi^4} \left[ \frac{v}{x} - 2 \mathcal{L}_v \right] - \frac{m_c^3(1-b^2) \langle \bar{s}Gs \rangle}{3^2 \times 2^8 \pi^4} \left[ v \left( 42x + 7 - \frac{40}{x} \right) + 6 \mathcal{L}_v \left( 14x^2 + 3 + \frac{2}{x} \right) \right] \\
&\quad + \frac{m_s m_c^2(1+b^2) \langle \bar{q}Gq \rangle}{2^6 \pi^4} v - \frac{m_s m_c^2(1+b^2) \langle \bar{s}Gs \rangle}{3^2 \times 2^9 \pi^4} \left[ v \left( 18x - 5 - \frac{4}{x} \right) + 18 \mathcal{L}_v(2x^2 + 1) \right], \\
\rho^{\langle \bar{q}q \rangle^2}(t) &= \frac{\langle \bar{q}q \rangle \langle \bar{s}s \rangle}{48 \pi^2} v \left[ 4m_c^2(1+b^2) - m_s m_c(1-b^2) \left( 1 + \frac{m_c^2 \tau}{x} \right) \right]. \tag{A8}
\end{aligned}$$



- [1] M. Gell-Mann, *Phys. Lett.* **8**, 214 (1964).
- [2] G. Zweig, Reports No. CERN-TH-401 and No. TH-412, 1964; in *Developments in Quark Theory of Hadrons*, Vol. 1, 1964/1978, edited by D. B. Lichtenberg and S. P. Rosen (Hadronic Press, MA, 1980).
- [3] G. C. Rossi and G. Veneziano, *Nucl. Phys.* **B123**, 507 (1977); arXiv:2011.09774.
- [4] R. L. Jaffe, *Phys. Rev. D* **15**, 267 (1977); *Phys. Rep.* **409**, 1 (2005).
- [5] J. D. Weinstein and N. Isgur, *Phys. Rev. D* **27**, 588 (1983).
- [6] N. N. Achasov, S. A. Devyanin, and G. N. Shestakov, *Sov. J. Nucl. Phys.* **32**, 566 (1980).
- [7] G. 't Hooft, G. Isidori, L. Maiani, A. D. Polosa, and V. Riquer, *Phys. Lett. B* **662**, 424 (2008).
- [8] J. I. Latorre and P. Pascual, *J. Phys. G* **11**, L231 (1985); S. Narison, *Phys. Lett. B* **175**, 88 (1986).
- [9] S. Narison and G. Veneziano, *Int. J. Mod. Phys. A* **04**, 2751 (1989); A. Bramon and S. Narison, *Mod. Phys. Lett. A* **04**, 1113 (1989).
- [10] S. Narison, *Nucl. Phys.* **B509**, 312 (1998); *Nucl. Phys. B, Proc. Suppl.* **64**, 210 (1998).
- [11] P. Minkowski and W. Ochs, *Eur. Phys. J. C* **9**, 283 (1999).
- [12] G. Mennessier, S. Narison, and W. Ochs, *Phys. Lett. B* **665**, 205 (2008); G. Mennessier, S. Narison, and X.-G. Wang, *Phys. Lett. B* **696**, 40 (2011).
- [13] L. WU, arXiv:2012.15473
- [14] R. M. Albuquerque, J. M. Dias, K. P. Khemchandani, A. M. Torres, F. S. Navarra, M. Nielsen, and C. M. Zanetti, *J. Phys. G* **46**, 093002 (2019).
- [15] A. Ali, L. Maiani, and A. D. Polosa, *Multiquark hadrons* (Cambridge University Press, Cambridge, England, 2019), ISBN 9781316761465, <https://doi.org/10.1017/9781316761465>.
- [16] J.-M. Richard, *Few Body Syst.* **57**, 1185 (2016), QCD20-Montpellier 27-30 october 2020.
- [17] E. S. Swanson, *Phys. Rep.* **429**, 243 (2006), QCD20-Montpellier 27-30 october 2020.
- [18] H. G. Dosch, QCD20-Montpellier 27-30 october 2020.
- [19] H. X. Chen, W. Chen, X. Liu, and S.-L. Zhu, *Phys. Rep.* **639**, 1 (2016).
- [20] F. K. Guo, C. Hanhart, U.-G. Meißner, Q. Wang, Q. Zhao, and B.-S. Zou, *Rev. Mod. Phys.* **90**, 015004 (2018).
- [21] N. Brambilla, S. Eidelman, C. Hanhart, A. Nefediev, C.-P. Shen, C. E. Thomas, A. Vairo, and C.-Z. Yuan, *Phys. Rep.* **873**, 1 (2020).
- [22] R. M. Albuquerque *et al.*, *Nucl. Part. Phys. Proc.* **300–302**, 186 (2018); *Int. J. Mod. Phys. A* **31**, 1650093 (2016); *Phys. Lett. B* **715**, 129 (2012).
- [23] R. M. Albuquerque, S. Narison, D. Rabetiarivony, and G. Randriamanatrika, *Int. J. Mod. Phys. A* **33**, 1850082 (2018); *Nucl. Part. Phys. Proc.* **282–284**, 83 (2017).
- [24] R. M. Albuquerque, S. Narison, F. Fanomezana, A. Rabemananjara, D. Rabetiarivony, and G. Randriamanatrika, *Int. J. Mod. Phys. A* **31**, 1650196 (2016).
- [25] M. A. Shifman, A. I. Vainshtein, and V. I. Zakharov, *Nucl. Phys.* **B147**, 385 (1979); **B147**, 448 (1979).
- [26] V. I. Zakharov, *Int. J. Mod. Phys. A* **14**, 4865 (1999).
- [27] S. Narison, *World Sci. Lect. Notes Phys.* **26**, 1 (1989), ISBN 9780521037310.
- [28] S. Narison, *Cambridge Monogr. Part. Phys., Nucl. Phys., Cosmol.* **17**, 1 (2004).
- [29] S. Narison, *Phys. Rep.* **84**, 263 (1982); *Acta Phys. Pol. B* **26**, 687 (1995); *Riv. Nuovo Cimento* **10N2**, 1 (1987); *Nucl. Part. Phys. Proc.* **258–259**, 189 (2015).
- [30] B. L. Ioffe, *Prog. Part. Nucl. Phys.* **56**, 232 (2006).
- [31] L. J. Reinders, H. Rubinstein, and S. Yazaki, *Phys. Rep.* **127**, 1 (1985).
- [32] E. de Rafael, arXiv:hep-ph/9802448.
- [33] R. A. Bertlmann, *Acta Phys. Austriaca* **53**, 305 (1981).
- [34] F. J. Yndurain, *The Theory of Quark and Gluon Interactions*, 3rd ed. (Springer, New York, 1999).
- [35] P. Pascual and R. Tarrach, *QCD: Renormalization for Practitioner* (Springer, New York, 1984).
- [36] H. G. Dosch, *Non-Perturbative Methods*, edited by S. Narison (World Scientific, Singapore, 1985).
- [37] P. Colangelo and A. Khodjamirian, *At the Frontier of Particle Physics: Handbook of QCD, 1495*, edited by M. Shifman (World Scientific, Singapore, 2001).
- [38] J. S. Bell and R. A. Bertlmann, *Nucl. Phys.* **B177**, 218 (1981); **B187**, 285 (1981).
- [39] C. Becchi, S. Narison, E. de Rafael, and F. J. Yndurain, *Z. Phys. C* **8**, 335 (1981).
- [40] S. Narison and E. de Rafael, *Phys. Lett. B* **522**, 266 (2001).
- [41] R. Aaij *et al.* (LHCb Collaboration), *Sci. Bull.* **65**, 1983 (2020).
- [42] R. M. Albuquerque, S. Narison, A. Rabemananjara, D. Rabetiarivony, and G. Randriamanatrika, *Phys. Rev. D* **102**, 094001 (2020); arXiv:2102.08776.
- [43] R. Aaij *et al.* (LHCb Collaboration), *Phys. Rev. Lett.* **125**, 242001 (2020); *Phys. Rev. D* **102**, 112003 (2020).
- [44] R. Albuquerque, S. Narison, D. Rabetiarivony, and G. Randriamanatrika, *Nucl. Phys.* **A1007**, 122113 (2021); arXiv:2102.04622.
- [45] M. Ablikim *et al.* (BESIII Collaboration), *Phys. Rev. Lett.* **126**, 102001 (2021).
- [46] S. Narison and R. Tarrach, *Phys. Lett.* **125B**, 217 (1983).
- [47] W. Lucha, D. Melikhov, and H. Sazdjian, *Phys. Rev. D* **100**, 014010 (2019); **100**, 074029 (2019).
- [48] G. Launer, S. Narison, and R. Tarrach, *Z. Phys. C* **26**, 433 (1984).
- [49] R. A. Bertlmann, G. Launer, and E. de Rafael, *Nucl. Phys.* **B250**, 61 (1985).
- [50] S. Narison, *Phys. Lett. B* **673**, 30 (2009).
- [51] Y. Chung, H. G. Dosch, M. Kremer, and D. Schall, *Z. Phys. C* **25**, 151 (1984).
- [52] H. G. Dosch, M. Jamin, and S. Narison, *Phys. Lett. B* **220**, 251 (1989).
- [53] E. V. Shuryak, *Phys. Rep.* **115**, 151 (1984); T. Schafer and E. V. Shuryak, *Rev. Mod. Phys.* **70**, 323 (1998).
- [54] S. Narison, *Phys. Lett. B* **693**, 559 (2010); **705**, 544(E) (2011).
- [55] S. Narison, *Phys. Lett. B* **706**, 412 (2012).
- [56] S. Narison, *Phys. Lett. B* **707**, 259 (2012).
- [57] A. Pich and E. de Rafael, *Phys. Lett.* **158B**, 477 (1985).
- [58] S. Narison and A. Pivovarov, *Phys. Lett. B* **327**, 341 (1994).
- [59] K. Hagiwara, S. Narison, and D. Namura, *Phys. Lett. B* **540**, 233 (2002).
- [60] W. Lucha, D. Melikov, and H. Sadjian, *Phys. Rev. D* **103**, 014012 (2021).

- [61] D. J. Broadhurst, *Phys. Lett.* **101B**, 423 (1981).
- [62] K. G. Chetyrkin and M. Steinhauser, *Phys. Lett. B* **502**, 104 (2001).
- [63] P. Gelhausen, A. Khodjamirian, A. A. Pivovarov, and D. Rosenthal, *Phys. Rev. D* **88**, 014015 (2013); **89**, 099901(E) (2014); **91**, 099901(E) (2015).
- [64] S. Narison, *Int. J. Mod. Phys. A* **33**, 1850045 (2018); **33**, 1850045(A) (2018) and references therein.
- [65] P. A. Zyla *et al.* (Particle Data Group), *Prog. Theor. Exp. Phys.* **2020**, 083C01 (2020).
- [66] S. Narison, arXiv:1812.09360.
- [67] S. Narison, arXiv:2101.12579; *Nucl. Part. Phys. Proc.* **300–302**, 153 (2018).
- [68] S. Narison, *Phys. Lett. B* **802**, 135221 (2020); **784**, 261 (2018).
- [69] S. Narison, *Phys. Lett. B* **718**, 1321 (2013).
- [70] S. Narison, *Int. J. Mod. Phys. A* **30**, 1550116 (2015); *Phys. Lett. B* **738**, 346 (2014).
- [71] R. M. Albuquerque and S. Narison, *Phys. Lett. B* **694**, 217 (2010); R. M. Albuquerque, S. Narison, and M. Nielsen, *Phys. Lett. B* **684**, 236 (2010).
- [72] B. L. Ioffe, *Nucl. Phys.* **B188**, 317 (1981); **B191**, 591(E) (1981).
- [73] A. A. Ovchinnikov and A. A. Pivovarov, *Yad. Fiz.* **48**, 1135 (1988).
- [74] S. Narison, *Phys. Lett. B* **605**, 319 (2005).
- [75] J. Bijnens, J. Prades, and E. de Rafael, *Phys. Lett. B* **348**, 226 (1995).
- [76] M. A. Shifman, *At the Frontier of Particle Physics: Handbook of QCD, 1447*, edited by M. Shifman (World Scientific, Singapore, 2001).
- [77] O. Catà, M. Golterman, and S. Peris, *Phys. Rev. D* **77**, 093006 (2008); D. Boito, I. Caprini, M. Golterman, K. Maltman, and S. Peris, *Phys. Rev. D* **97**, 054007 (2018).
- [78] A. Pich and A. Rodriguez-Sanchez, *Phys. Rev. D* **94**, 034027 (2016).
- [79] A. Bondar *et al.* (Belle Collaboration), *Phys. Rev. Lett.* **108**, 122001 (2012); Z. Liu *et al.*, *Phys. Rev. Lett.* **110**, 252002 (2013); **111**, 019901(E) (2013).
- [80] M. Ablikim *et al.* (BESIII Collaboration), *Phys. Rev. Lett.* **110**, 252001 (2013).
- [81] M. Ablikim *et al.* (BESIII Collaboration), *Phys. Rev. Lett.* **111**, 242001 (2013).
- [82] M. Ablikim *et al.* (BESIII Collaboration), *Phys. Rev. Lett.* **112**, 132001 (2014); **115**, 182002 (2015).
- [83] X. L. Wang *et al.* (Belle Collaboration), *Phys. Rev. D* **91**, 112007 (2015).
- [84] M. Ablikim *et al.* (BESIII Collaboration), *Phys. Rev. Lett.* **115**, 222002 (2015).
- [85] S. K. Choi *et al.* (Belle Collaboration), *Phys. Rev. Lett.* **100**, 142001 (2008).
- [86] R. Aaij *et al.* (LHCb Collaboration), *Phys. Rev. Lett.* **112**, 222002 (2014).
- [87] Z. G. Wang, *Phys. Rev. D* **101**, 074011 (2020) and references therein.
- [88] Z. G. Wang and T. Huang, *Phys. Rev. D* **89**, 054019 (2014).
- [89] S. Narison and V. I. Zakharov, *Phys. Lett. B* **679**, 355 (2009).
- [90] K. G. Chetyrkin, S. Narison, and V. I. Zakharov, *Nucl. Phys.* **B550**, 353 (1999).
- [91] S. Narison and V. I. Zakharov, *Phys. Lett. B* **522**, 266 (2001).
- [92] For reviews, see, e.g., V. I. Zakharov, *Nucl. Phys. B, Proc. Suppl.* **164**, 240 (2007); S. Narison, *Nucl. Phys. B, Proc. Suppl.* **164**, 225 (2007).
- [93] S. Narison, *Phys. Lett. B* **718**, 1321 (2013); *Nucl. Part. Phys. Proc.* **270–272**, 143 (2016); *Int. J. Mod. Phys. A* **30**, 1550116 (2015).
- [94] R. F. Lebed and A. D. Polosa, *Phys. Rev. D* **93**, 094024 (2016).
- [95] Z.-G. Wang, *Commun. Theor. Phys.* **63**, 325 (2015).
- [96] V. De Alfaro *et al.*, *Current in Hadron Physics* (Elsevier, North-Holland, 1973), ISBN 0 7204 0212 3.
- [97] X. Jin *et al.*, arXiv:2011.12230; M.-C. Du, Q. Wang, and Q. Zhao, arXiv:2011.09225; L. Meng, B. Wang, and S.-L. Zhu, *Phys. Rev. D* **102**, 111502 (2020); Z. Yang *et al.*, arXiv:2011.08725; M.-Z. Liu *et al.*, arXiv:2011.08720; Z.-H. Guo and J. A. Oller, *Phys. Rev. D* **103**, 054021 (2021); N. Ikeno, R. Molina, and E. Oset, *Phys. Lett. B* **814**, 136120 (2021).
- [98] S. H. Lee, M. Nielsen, and U. Wiedner, *J. Korean Phys. Soc.* **55**, 424 (2009); J. M. Dias, F. S. Navarra, M. Nielsen, and C. M. Zanetti, *Phys. Rev. D* **88**, 016004 (2013).
- [99] B.-D. Wan and C.-F. Qiao, arXiv:2011.08747; Q. N. Wang, W. Chen, and H.-X. Chen, arXiv:2011.10495; Z.-G. Wang, arXiv:2011.10959.